Homology, Homotopy and Applications, vol. ??(??), ????, pp.1Doc-Start–33

EQUIVARIANT COSHEAVES AND GRAPHIC STATICS

ZOE COOPERBAND, MIGUEL LOPEZ AND BERND SCHULZE

Abstract

This work extends the theory of reciprocal diagrams in graphic statics to frameworks that are invariant under finite group actions by utilizing the homology and representation theory of cellular cosheaves, recent tools from applied algebraic topology. By introducing the structure of an equivariant cellular cosheaf, we prove that pairs of self-stresses and reciprocal diagrams of symmetric frameworks are classified by the irreducible representations of the underlying group. We further derive the symmetry-aligned Euler characteristics of a finite dimensional equivariant chain complex, which for the force cosheaf yields a new formulation of the symmetry-adapted Maxwell counting rule for detecting symmetric self-stresses and kinematic degrees of freedom in frameworks. A freely available program is used to implement the relevant cosheaf homologies and illustrate the theory with examples.

1. Introduction

Graphic statics is a geometric toolbox for analyzing the relationship between the form of a bar-joint framework and its internal force loading. The theory dates back to classical work of Maxwell and Cremona [33, 15] and has been widely used for designing and modeling various types of real-world structures. Building on earlier work by Rankine and others, they discovered that for a plane framework, there is an equivalence between its self-stresses (or equilibrium stresses) and its reciprocal diagrams (or force diagrams), which realize the dual of the original graph as frameworks with bar lengths determined by the stress coefficients. See Figure 1 for an example.

They also found that the vertical projection of a spatial polyhedron into the plane yields a framework with a self-stress. In 1982 Whiteley established the converse of this result by showing that every self-stressed plane framework on a polyhedral graph can be vertically lifted to a polyhedron in 3-space (also known as a "discrete Airy stress function polyhedron" in engineering), where the changes in slope along edges are encoded by the corresponding stress coefficients [44]. See also Crapo and Whiteley [14]. Since then, the Maxwell-Cremona correspondence has been applied to the solution of numerous problems in polyhedral combinatorics, and discrete and computational geometry. See e.g. [9, 27, 43].

2020 Mathematics Subject Classification: 52C25, 55N30, 20C35

Key words and phrases: equilibrium stress, reciprocal diagram, graphic statics, cosheaf homology, symmetry, equivariant cosheaf.

Article available at `http://dx.doi.org/10.4310/HHA.????.v??.n??.a?`

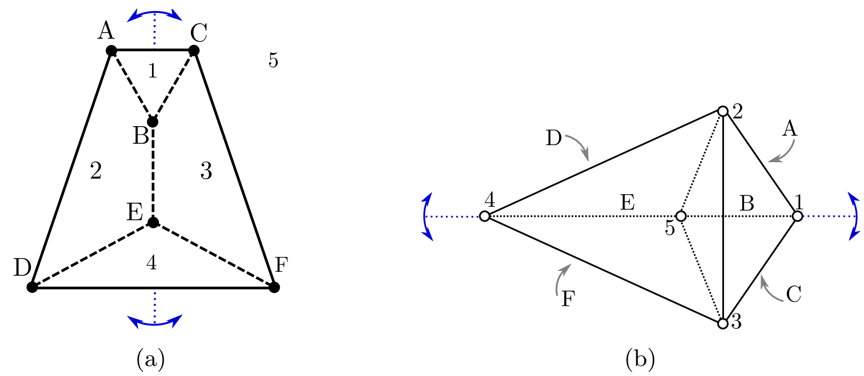

Figure 1: A planar framework in *Desargues configuration* with a self-stress and vertical mirror-symmetry (a) and its corresponding mirror-symmetric reciprocal diagram, where corresponding edges are parallel (b). The "transformation" of the mirror from vertical to horizontal is a consequence of Remark 3.10. Reflections in dashed mirror lines are indicated by curved double arrows. Solid vs dashed edges in (a) indicate tension vs compression in elements.

Increased interest in the design of material-efficient structures in engineering, such as gridshell roofs or cable net structures, has heralded a surge of interest in this theory. The visual nature of force-form duality allows an integrated analysis early into the design process, crucial for finding optimal designs. Modern computational tools play a key role here, as they allow quick visualisations of these relationships. Techniques from graphic statics have recently also found new applications in control theory [36] and materials science [21].

Recently, there has been an explosion of results regarding the rigidity, flexibility and stressability of *symmetric* frameworks. See e.g. [11, 40] for an introduction to the theory and a summary of results. Much of this work has been motivated by problems from the applied sciences and industry, where symmetry is utilized by both man-made and natural structures for stability, construction, and aesthetics. For gridshell roofs, increasing the dimensionality of the space of self-stresses can reduce the volume of material needed to construct the load-bearing structure [38]. By associating the self-stresses of different symmetry types to irreducible representations of the symmetry group of the structure[1], new tools for designing and analyzing gridshell structures were recently obtained in [38, 35]. Using a similar approach, refined relations between self-stresses and motions of different symmetries in form and force diagrams were established in [37].

Recently, a homological description of 2D graphic statics was given in [12] affirming algebraic topology as a useful theory for structural engineering. This work built upon the observation made in [12] that the self-stresses of a framework can be encoded

[1]Self-stresses with both symmetric and anti-symmetric sign patterns for the stress coefficients play an important role in the design of gridshells. While fully-symmetric self-stresses relate to symmetric vertical loadings of the gridshell (such as self-weight), anti-symmetric self-stresses relate to anti-symmetric loadings, such as uneven gravity loads arising from drifted snow, for example.

with a tool called a cellular cosheaf. Developed and popularized by the theses of Shepard [41] and Curry [16], cellular sheaves and cosheaves have rapidly found wide applications in areas such as network coding [20], optimization [23], space networks [42], opinion dynamics [24], and many more. Recently, there have been numerous exciting applications in machine learning, where the sheaf Laplacian [25] fittingly encodes network data diffusion. This work incidentally describes data equivariance over networks and cell-complexes, bridging the gap towards advances in *equivariant* and *convolutional* neural networks [8, 5].

Cosheaves embody the *finite element* approach, namely breaking a physical system into smaller units which relate to other units by constraint equations. Finite elements, when framed in terms of cosheaf stalks and extension maps, have access to the wide array of formal methods from homological algebra. The concept of moving from local to global equilibria is paralleled with moving from local to global sections in sheaves, bundles, and other algebraic constructions. This paper is an early description of such methods for *homological engineering*, or designing chain complexes and homology spaces to model the constraints and degrees of freedom of complex physical systems.

1.1. Contributions

In the present article, we utilize representation theory and computational homology to gain deeper insights into 2D symmetric graphic statics. (The elementary details on representations are contained in the Appendix A.) We show that group actions on frameworks give rise to group actions on cosheaves whose homology encodes structural information. The *force and position cosheaves*, encoding the space of self-stresses and reciprocal coordinates respectively, both pass to the group action. We develop the *Euler characteristic* of irreducible cosheaf characters to reformulate Maxwell's counting rule for symmetric frameworks (Theorem 4.5) and to provide a new proof of this result. We then prove our main theorem, which says that the Maxwell-Cremona equivalence between self-stresses of a framework and its reciprocal diagrams not only occurs over symmetric frameworks, but that this equivalence also respects the underlying irreducible representations (Theorem 4.7).

As a consequence of Theorem 4.7, self-stress and reciprocal diagram pairs can be aligned and organized by their underlying symmetry. Moreover, this theory can be used to decompose reciprocal diagrams of self-stressed frameworks with point group symmetry G into diagrams of basic symmetry types corresponding to irreducible representations of G. See Appendix B for a detailed example. While Theorem 4.7 is simple to state, it generalizes previous works [37, 38] with an advanced method extending to any finite symmetry group and symmetry type. This general result had been out of reach with previous methods, but becomes accessible through our novel cosheaf-theoretic approach, which provides the first mathematical proof of these symmetry relationships in graphic statics.

In structural engineering, our results enable a targeted stress analysis of gridshell roofs and related structures based on specific symmetry types to enhance stability and optimize load distribution. While our methods apply to arbitrary finite symmetry groups, we focus our examples on small dihedral groups, which are particularly relevant in engineering applications. Computationally, the advantage is that for a stress analysis of a particular symmetry type, we can reduce the system by effectively examining a quotient structure, significantly simplifying the problem. In fact, the structural and matrix complexity is roughly divided by the order of the symmetry group, since we are typically working with symmetric structures where the group action is free on most members. See also Appendix B.

Equivariant cellular cosheaves, as introduced here, are closely related to equivariant coefficient systems over simplicial complexes as developed in [4]. Equivariant sheaves have found use in equivariant homotopy theory [3], and equivariant homology is an active sub-field of algebraic topology [34], but to the authors' knowledge, this is the first description and application of this particular structure. We expect equivariant cosheaves to be useful more broadly in symmetric rigidity theory [40], including applications to the first-order rigidity of frameworks with phase symmetry [39] and other contexts where symmetry-adapted decompositions can simplify structural analysis and provide deeper insights.

The paper is organized as follows: In Section 2 we provide the necessary background on graphic statics cellular cosheaves. In Section 3 we introduce the notion of an *equivariant* cellular cosheaf, combining the theories of the previous section with group representation theory. Section 4 focuses on the irreducible components of the homology relations, and in particular develops the graphic statics relations of irreducibles. Finally, in Section 5 we discuss some avenues for future work. The Appendix A covers the necessary standard representation theory. For greater clarity, thorough computations on a simple framework are carried out in Appendix B.

The figures in this paper were developed using Python code that is freely available at the following link: https://github.com/zcooperband/EquivariantGraphicStatics. In the linked project, the relevant cosheaf homologies are implemented using matrix methods, and equivariant irreducible self-stress reciprocal diagram pairs are extracted. The project contains several prepared sample frameworks and tests for quick verification of commutativity of diagrams of the form (18).

2. Statics, Graphic Statics, and Cosheaves

While in structural engineering it is common to merge the abstract/combinatorial and geometric characteristics of a pin-jointed truss model, it is useful to distinguish between the two. Discounting geometric singularities, many algebraic properties of a truss are invariant under changes in geometry. The underlying combinatorial structure is that of a cell complex.

A (finite, regular, CW) *cell complex* is a topological space X partitioned into a finite number of cells $\{c\}$, where each cell c is homeomorphic to a topological disk of some dimension[2]. We say cells c and d are *incident* and write $c \lhd d$ if c is a lower dimensional cell on the boundary of the closure of d.

A *signed incidence relation* on a cell complex X assigns to each pair c, d of cells of X a value $[c : d] \in \{0, \pm 1\}$, so that the following properties are satisfied:

- (Adjacency) $[c : d] \neq 0$ if and only if $c \lhd d$ and $\dim c + 1 = \dim d$.
- (Directed Edges) $[u : e][v : e] = -1$ for an edge with incident vertices $u, v \lhd e$.
- (Regularity) For any $b \lhd d$, $\sum_c [b : c][c : d] = 0$.

[2] Moreover, cells must have "nice intersections"; for a complete definition of a regular (CW) complex see [16]. For the purposes of this paper, systems of polyhedra are regular cell complexes.

A signed incidence relation encodes the consistency of local orientations over cells. When the orientation of two incident cells $c \lhd d$ agree, such as when a directed edge "points towards" a vertex, we set $[c : d] = +1$; otherwise we set $[c : d] = -1$.

A *framework* (G, p) in the plane $\mathbb{R}^2$ is a graph G with sets of vertices $\mathscr{V}$ and edges $\mathscr{E}$ together with a *realization* map $p : \mathscr{V} \to \mathbb{R}^2$ that assigns each vertex v a geometric position $p_v = p(v) \in \mathbb{R}^2$. We typically require that p be locally injective, meaning that for every edge with endpoints $u, v \lhd e$, we have $p_u \neq p_v$ (although in reciprocal diagrams of frameworks this property may be lost). A framework (G, p) is *planar* if its edges, embedded in $\mathbb{R}^2$ as straight lines, do not intersect anywhere except at their endpoints. A planar framework induces a cell complex X, which we may write as $X = (\mathscr{V}, \mathscr{E}, \mathscr{F})$ where $\mathscr{F}$ is the set of faces that naturally correspond to the connected components of the complement of the union of the geometric edges. Dually, every two-dimensional cell complex realized in $\mathbb{R}^2$ determines a framework (which may have overlapping faces). In the following, we will often abuse terminology slightly and call (X, p) a framework in $\mathbb{R}^2$.

Every framework models a *pin-jointed truss* in the plane. This is a geometric model of a physical truss, where the nodes allow rotations in any direction of the space and the truss members are loaded in pure axial tension or compression. A *stress* over a framework (X, p) is an assignment of a real-valued scalar w_e to each edge e encoding the internal tension or compression force over that edge. A *self-stress* (or *equilibrium stress*) w on a framework (X, p) is a stress that satisfies the following equation[3] at every vertex v

$$\sum_{\{v \lhd e \rhd u : v \neq u\}} w_e(p_v - p_u) = 0, \tag{1}$$

the sum being over the edges e that are incident with v.

Equilibrium stresses encapsulate the condition that the truss is in force *equilibrium* and are of vital importance to structural engineering statics. In the next section, we show that equilibrium stresses are an instance of a much more general phenomenon.

2.1. Cellular Cosheaves

In a variety of engineering applications, vector valued data is assigned to the cells of a cell complex. This data can be forces, kinematic motions, positions, and other geometric-algebraic data. Cosheaves are mathematically precise and concise formulations of these distributed data structures.

Definition 2.1 (Cellular cosheaf)**.** Fixing a field k, a (k-valued cellular) *cosheaf* $\mathcal{K}$ over a cell complex X consists of the following data. Each cell $c \in X$ is assigned a finite dimensional vector space $\mathcal{K}_c \cong k^n$, for some $n \in \mathbb{N}$, called the *stalk at* c. When cells $c \lhd d$ are incident, a linear *extension map* is assigned between stalks $\mathcal{K}_{d \rhd c} : \mathcal{K}_d \to \mathcal{K}_c$. Cosheaves are functors, meaning that $\mathcal{K}_{c \rhd b} \circ \mathcal{K}_{d \rhd c} = \mathcal{K}_{d \rhd b}$ and $\mathcal{K}_{c \rhd c} = \mathrm{id}$ for incident cells $b \lhd c \lhd d$.

We fix the field of all cellular cosheaves to be $\mathbb{R}$ or $\mathbb{C}$. One thinks of a cosheaf as a blueprint for local algebraic data, describing what data is attached to which cell and

[3]Here the value w_e corresponds to a tension/compression force scaled by the length of the edge $\|p_v - p_u\|$.

how these relate. However, to detect global algebraic structure, we use the blueprint and build a computational machine known as a chain complex.

Definition 2.2 (Cosheaf chain complex)**.** The space of *i-chains* of a cosheaf $\mathcal{K}$ over a cell complex X is the direct sum of stalks

$$C_i\mathcal{K} = \bigoplus_{\dim c = i} \mathcal{K}_c.$$

The *boundary* of an i-chain x is the $i-1$ dimensional chain ∂x with component

$$(\partial x)_c = \sum_{c \lhd d} [c:d]\mathcal{K}_{d \rhd c} x_d$$

at the $i-1$ dimensional cell c. Note that $\partial x = 0$ if x is a 0-chain. From the regularity property of signed incidence relations, it follows that $\partial \circ \partial = 0$ and hence

$$\dots C_{i+1}\mathcal{K} \xrightarrow{\partial_{i+1}} C_i\mathcal{K} \xrightarrow{\partial_i} C_{i-1}\mathcal{K} \to \dots \tag{2}$$

is a *chain complex* denoted $C\mathcal{K}$.

Certain practical necessities, such as the orientations of cells, are necessary for computations and amount to a choice of basis for chains. This motivates decoupling the cosheaf abstraction from its computational aspects of its underlying chain complex, primarily used to compute its *homology*.

Definition 2.3 (Cosheaf homology)**.** Let $\mathcal{K}$ be a cosheaf over a cell complex X. We say an i-chain $x \in C_i\mathcal{K}$ is a *cycle* if $\partial_i(x) = 0$. The i-th *cosheaf homology* of the chain complex $C\mathcal{K}$ is

$$H_i\mathcal{K} = \ker \partial_i / \operatorname{im} \partial_{i+1}$$

i.e. the space of quotients of cycles by boundaries of higher dimensional chains.

Example 2.4 (Constant cosheaves). Let V be a finite dimensional vector space. The *constant cosheaf* $\overline{V}$ over a cell complex X has identical stalks $\overline{V}_c = V$ for all cells c and identity extension maps $\overline{V}_{d \rhd c} = \mathrm{id}$. The homology of $\overline{V}$ is isomorphic to m copies of cellular homology with $\dim H\overline{V} = m \dim H(X;k)$ where $m = \dim V$.

Example 2.5 (The force cosheaf). The following force cosheaf encodes the forces within an axially loaded pin-jointed truss as well as equilibrium stresses of the truss. This cosheaf is non-trivial and has been defined and developed previously in the context of graphic statics [12, 13].

Fix a planar framework (X,p) in $\mathbb{R}^2$. The force cosheaf $\mathcal{F}$ over (X,p) has stalks $\mathcal{F}_e = \mathbb{R}$ encoding the axial force in an edge e and $\mathcal{F}_v = \mathbb{R}^2$ encoding the space of external forces at each joint. The stalks over the faces of X vanish. Both extension maps $\mathcal{F}_{e \rhd u}$ and $\mathcal{F}_{e \rhd v}$ send $1 \in \mathcal{F}_e$ to the same vector[4]

$$[v:e](p_v - p_u) = [u:e](p_u - p_v). \tag{3}$$

The boundary map of the force cosheaf $\partial : C_1\mathcal{F} \to C_0\mathcal{F}$ can be represented as a size $2|V| \times |E|$ matrix known as the *equilibrium matrix*. Note that the equilibrium matrix

[4]This assignment dictates that $1 \in \mathcal{F}_e$ corresponds to the edge being in compression scaled by the length of the edge. If we were to wish for the basis element $1 \in \mathcal{F}_e$ to correspond to a tension value, we would simply set $\mathcal{F}_{e \lhd v}(1) = \mathcal{F}_{e \lhd u}(1) = [v:e](p_u - p_v)$.

is the transpose of the classical rigidity matrix from geometric rigidity theory [11]. The kernel of ∂ is the first homology $H_1\mathcal{F}$, the vector space of equilibrium stresses of the structure. To confirm this, we expand the boundary matrix at a chain $w \in C_1\mathcal{F}$

$$(\partial w)_v = \sum_{v \lhd e} [v:e]\mathcal{F}_{e \rhd v} w_e = \sum_{\{v \lhd e \rhd u : v \neq u\}} [v:e]^2 (p_v - p_u) w_e \tag{4}$$

which is zero at all vertices v exactly when w is an equilibrium stress following Equation (1). The cokernel of ∂ is the zeroth homology $H_0\mathcal{F} = C_0\mathcal{F}/\operatorname{im}\partial$, interpreted as the space of *infinitesimal motions* of the framework. These include the trivial infinitesimal motions corresponding to rigid body motions (rotation and translation) as well as the non-trivial infinitesimal motions (mechanisms).

2.2. Maps Between Cosheaves

An *exact sequence* of vector spaces is a sequence of vector spaces and linear maps

$$\cdots \to V_3 \xrightarrow{f_2} V_2 \xrightarrow{f_1} V_1 \xrightarrow{f_0} V_0 \xrightarrow{f_{-1}} V_{-1} \to \ldots \tag{5}$$

where for each index the maps satisfy $\operatorname{im} f_i = \ker f_{i-1}$. A *short exact sequence* is of form (5) where $V_i = 0$ except at indices $i = 0, 1, 2$. Then the map f_1 would be injective and the map f_0 surjective with isomorphism $V_0 \oplus V_2 \cong V_1$.

Let $\mathcal{K}$ and $\mathcal{L}$ be cosheaves over a cell complex X. A *cosheaf map* $\phi : \mathcal{K} \to \mathcal{L}$ is comprised of component maps between stalks $\phi_c : \mathcal{K}_c \to \mathcal{L}_c$ such that the following diagram commutes

$$\begin{tikzcd} \mathcal{K}_d \arrow[r, "\phi_d"] \arrow[d, "\mathcal{K}_{d \rhd c}"] & \mathcal{L}_d \arrow[d, "\mathcal{L}_{d \rhd c}"] \\ \mathcal{K}_c \arrow[r, "\phi_c"] & \mathcal{L}_c \end{tikzcd} \tag{6}$$

for every pair of incident cells $c \lhd d$. Cosheaf maps induce maps on chain complexes $\phi : C\mathcal{K} \to C\mathcal{L}$ comprised of the constituent maps. A *short exact sequence of cosheaves* $0 \to \mathcal{K} \to \mathcal{L} \to \mathcal{M} \to 0$ has an induced short exact sequence of cosheaf maps

$$0 \to C\mathcal{K} \xrightarrow{\phi} C\mathcal{L} \xrightarrow{\psi} C\mathcal{M} \to 0 \tag{7}$$

such that the induced sequence at each stalk

$$0 \to \mathcal{K}_c \xrightarrow{\phi_c} \mathcal{L}_c \xrightarrow{\psi_c} \mathcal{M}_c \to 0 \tag{8}$$

is exact. All cosheaf stalks we will discuss are finite dimensional and we assume the underlying cell complex X has only a finite number of cells, so the sequence (7) is an exact sequence of finite dimensional vector spaces.

From any injective cosheaf map $\phi : \mathcal{K} \to \mathcal{L}$ we can construct the quotient cosheaf $\mathcal{L}/\phi\mathcal{K}$ with stalks $(\mathcal{L}/\phi\mathcal{K})_c = \mathcal{L}_c/\operatorname{im}\phi_c\mathcal{K}_c$. If each stalk $\mathcal{K}_c$ is considered as a subspace of the stalk $\mathcal{L}_c$ under the embedding ϕ_c, we may treat $\mathcal{K}$ as a sub-cosheaf of $\mathcal{L}$ and drop notation to $\mathcal{L}/\mathcal{K}$.

A short exact sequence of cosheaf maps induces maps on homology, and moreover we get a *long exact sequence in homology*

$$\cdots \to H_{i+1}\mathcal{L}/\mathcal{K} \xrightarrow{\vartheta} H_i\mathcal{K} \xrightarrow{\phi} H_i\mathcal{L} \xrightarrow{\psi} H_i\mathcal{L}/\mathcal{K} \xrightarrow{\vartheta} H_{i-1}\mathcal{K} \to \dots \tag{9}$$

where ϑ are *connecting homomorphisms*.

Example 2.6 (Planar graphic statics). Suppose (X, p) is a planar framework in $\mathbb{R}^2$. Both the force cosheaf $\mathcal{F}$ from Example (2.5) and the constant cosheaf $\overline{\mathbb{R}^2}$ are set over this framework (X, p). There is a natural injective map ϕ from $\mathcal{F}$ to $\overline{\mathbb{R}^2}$ which we now describe.

The map ϕ is the identity over vertices with $\phi_v : \mathcal{F}_v \to \overline{\mathbb{R}^2}_v$ equating stalks $\mathcal{F}_v = \mathbb{R}^2$ and $\overline{\mathbb{R}^2}_v = \mathbb{R}^2$. Then ϕ is injective over edges, where over an edge $u, v \lhd e$, $\phi_e : \mathcal{F}_e \to \overline{\mathbb{R}^2}$ sends[5] 1 to the vector $[u : e](p_u - p_v)$. By construction, ϕ is natural with

$$\mathrm{id} \circ \mathcal{F}_{e \rhd v} = \phi_v \circ \mathcal{F}_{e \rhd v} = \overline{\mathbb{R}^2}_{e \rhd v} \circ \phi_e = \mathrm{id} \circ \phi_e$$

and with a similar equation over the other incidence $u \lhd e$.

We assign the notation $\mathcal{P} := \overline{\mathbb{R}^2}/\phi\mathcal{F}$ for convenience, and let $\pi : \overline{\mathbb{R}^2} \to \mathcal{P}$ denote the cosheaf quotient map. We call $\mathcal{P}$ the *position cosheaf* dual to $\mathcal{F}$ because we will see that $\mathcal{P}$ encodes the positions of the dual vertices of reciprocal diagrams. Since trusses have trivial data over faces f, $\mathcal{F}_f = 0$ and $\mathcal{P}_f = \overline{\mathbb{R}^2}_f = \mathbb{R}^2$. Over an edge $u, v \lhd e$, we know that $\phi\mathcal{F}_e$ is the span of the vector $(p_u - p_v)$ and consequently $\mathcal{P}_e = \mathbb{R}^2/\mathrm{span}\{p_u - p_v\}$. Lastly, $\mathcal{P}_v = 0$ over vertices v.

In graphic statics, self-stresses of a planar framework $X = (\mathscr{V}, \mathscr{E}, \mathscr{F})$ are associated with *reciprocal diagrams*: realizations ξ of the dual cell complex $\tilde{X} = (\tilde{\mathscr{F}}, \tilde{\mathscr{E}}, \tilde{\mathscr{V}})$ such that an edge e is parallel with its dual $\tilde{e}$. See e.g. Figure 1. Abstractly, the position of a dual node $\tilde{f}$ is a coordinate in $\mathbb{R}^2$ which we encode by the map $\xi : \tilde{\mathscr{F}} \to \mathbb{R}^2$. The collection of these positions $\xi\tilde{\mathscr{F}}$ must satisfy the constraint that $\xi_{\tilde{f}} - \xi_{\tilde{g}}$ is parallel with the vector $p_u - p_v$ for any edge with vertex and face incidences $u, v \lhd e \lhd f, g$. Equivalently, $\xi_{\tilde{f}} - \xi_{\tilde{g}}$ is an element of $\mathrm{span}\{p_u - p_v\}$ and therefore

$$[\xi_{\tilde{f}} - \xi_{\tilde{g}}] = [0] \in \mathbb{R}^2/\mathrm{span}\{p_u - p_v\} = \mathcal{P}_e \tag{10}$$

is the zero class.

This is all to say the space of parallel reciprocal diagrams, encoded by realizations ξ over $\tilde{\mathscr{F}} \cong \mathscr{F}$ over vertices of the dual graph $\tilde{X}$, are elements of $H_2\mathcal{P}$. We see that ξ is a cycle if and only if Equation (10) is satisfied everywhere [12].

From the exact sequence of $\mathcal{F}$, $\overline{\mathbb{R}^2}$ and the quotient cosheaf $\mathcal{P}$ we have a segment of the long exact sequence

$$0 \to H_2\overline{\mathbb{R}^2} \to H_2\mathcal{P} \xrightarrow{\vartheta} H_1\mathcal{F} \xrightarrow{\phi} H_1\overline{\mathbb{R}^2} \to \dots \tag{11}$$

Since the framework is planar and hence X has spherical topology, $H_2X \cong \mathbb{R}$ and $H_1X = 0$. Consequently, the constant homology is determined as $H_2\overline{\mathbb{R}^2} \cong \mathbb{R}^2$ and $H_1\overline{\mathbb{R}^2} = 0$ and line (11) simplifies considerably. We find there is an isomorphism $\vartheta : H_2\mathcal{P}/\mathbb{R}^2 \to H_1\mathcal{F}$, meaning that the space of self-stresses of X is isomorphic to the space of parallel reciprocal diagrams of $\tilde{X}$ up to global translation.

[5] This assignment is the same as the extension maps $\mathcal{F}_{e \rhd u}$ and $\mathcal{F}_{e \rhd v}$.

In the above Example 2.6, we derived the position cosheaf purely from the force and constant cosheaves. The properties of any quotient cosheaf in general can be derived in a similar manner (by the universal property of quotients). This is critical because the problem of understanding quotient spaces (here reciprocal diagrams) is translated into an equivalent problem of understanding its precursors (here self-stresses and ambient space) which are often much more tractable.

3. Equivariant Cosheaves

We now integrate the theory of cellular cosheaves with that of finite group representations. (Basic results on the latter are provided in Appendix A.) This combination enables us to define equivariant cosheaves, which provide a framework for describing symmetric data assignments. We then focus on applications: symmetric force loading assignments and symmetric reciprocal frameworks.

Definition 3.1 (G-cell complex)**.** For a finite group G, a *G-cell complex* (X, α) is a cell complex X with a permutation action $\alpha : G \times X \to X$ on the set of cells of X satisfying:

- (Functorial) For any cell c, any $g, h \in G$, and $\epsilon \in G$ the identity element, we have $\alpha(g, \alpha(h, c)) = \alpha(gh, c)$ and $\alpha(\epsilon, c) = c$.
- (Equivariant) If $c \lhd d$ then $\alpha(g, c) \lhd \alpha(g, d)$.

Definition 3.2 (G-cosheaf)**.** Suppose that G is a finite group, (X, α) is a G-cell complex and $\mathcal{K}$ is a k-cosheaf over (X, α) such that $\mathcal{K}_c \cong \mathcal{K}_{gc}$ for every $g \in G$ and cell c. A *cosheaf representation* ρ is a family of group representations on each space of chains $\{\rho_i : G \to \mathrm{GL}_k(C_i\mathcal{K})\}$ such that:

(i) For every $g \in G$, $\rho_{i-1}(g) \circ \partial_i = \partial_i \circ \rho_i(g)$.

(ii) For x an i-chain, the value of $\rho_i(g)(x)$ at a cell gc depends only on x_c. In other words, there are isomorphisms for each cell, $\rho_c : G \to \mathrm{Orbit}(\mathcal{K}_c)$, such that $(\rho_i(g)(x))_{gc} = \rho_c(g)x_c$.

We say the pair $(\mathcal{K}, \rho)$ is a (k)*G-cosheaf.*

There are numerous observations we can make about G-cosheaves. From point (i), for each g, $\rho(g)$ is a G-chain complex[6] automorphism from $C\mathcal{K}$ to itself. This means each chain space $C_i\mathcal{K}$ is a G-module and the boundary maps ∂_i are G-homomorphisms. Utilizing point (ii) of Definition 3.2 and looking at the component of the boundary map corresponding to the incidence $c \lhd d$, we find that point (i) is

[6]A G-chain complex is a functor from G as a single object category to the category of chain complexes.

equivalent to the equation

$$\begin{aligned}(\rho_{i-1}(g)\circ\partial_i(x_d))_{gc} &= [c:d]\rho_c(g)\mathcal{K}_{d\rhd c}x_d\\ &= [gc:gd]\mathcal{K}_{gd\rhd gc}\rho_d(g)x_d\\ &= (\partial_i\circ\rho_i(g)(x_d))_{gc}.\end{aligned}\tag{12}$$

being satisfied everywhere. Consequently, the "local" components of the cosheaf representation ρ, $\{\rho_c\}$ satisfy the commutative diagram

$$\begin{tikzcd} \mathcal{K}_d \arrow[r, "\rho_d(g)"] \arrow[d, "\mathcal{K}_{d\rhd c}"'] & \mathcal{K}_{gd} \arrow[d, "\mathcal{K}_{gd\rhd gc}"] \\ \mathcal{K}_c \arrow[r, "\rho_c(g)"] & \mathcal{K}_{gc} \end{tikzcd}\tag{13}$$

up to sign, for every $g\in G$ and every incidence $c\lhd d$. Recalling diagram (6), the above diagram (13) is exactly the condition that $\rho(g)$ is a G-cosheaf map. Therefore, every G-cosheaf representation ρ is nearly a G-natural cosheaf automorphism[7], and is so up to sign (this is a point worthy of future investigation).

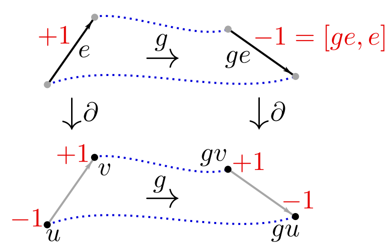

Figure 2: A sketch of the trivial representation ι over the constant cosheaf $\overline{\mathbb{R}}$, satisfying the constraint equation (12). The edge e changes orientation under the group action g, meaning $[ge,e]=-1$. The trivial representation ι does not detect cell geometry or embedding, only orientations.

Example 3.3 (Trivial constant G-cosheaves). Here we illustrate why a cosheaf representation may not be a G-indexed family of cosheaf maps. Permuting the underlying cell interferes with preservation of orientation and signs, even on the simplest cosheaves.

Suppose (X,α) is a G-cell complex and $\overline{\mathbb{R}^n}$ is a constant cosheaf over (X,α). The *trivial cosheaf representation* ι over $\overline{\mathbb{R}^n}$ is comprised of local maps $\iota_c(g)=[gc,c]\cdot\mathrm{id}$ for every $g\in G$ and cell c, where $[gc,c]\in\pm1$ measures orientation alignment between c and gc. We let $[gc,c]=+1$ if the orientation of c is reflected by the g action, or $[gc,c]=-1$ if the orientation of c is reversed. To satisfy Equation (12) we require

$$[gc,c][c:d]=[gc:gd][gd,d]\tag{14}$$

to hold true for all $c\lhd d$ and g. Requiring vertices to always have positive sign, $[gv,v]=+1$ for all v, an edge $u,v\lhd e$ changes sign and has $[ge,e]=-1$ when $[v:$

[7]We mean a functor from G as a single object category to the category of natural transformations of cosheaves to themselves.

$e][gv : ge] = -1$ (or equivalently $[u : e][gu : ge] = -1$). This sign change is demonstrated in Figure 2.

With this trivial cosheaf action ι, structure follows from the underlying permutation action α. Over the unit constant cosheaf $\overline{\mathbb{R}}$, each map $\iota_i(g) : C_i\overline{\mathbb{R}} \to C_i\overline{\mathbb{R}}$ is a signed permutation matrix with cells for basis elements. Abusing notation and declaring α_i to be a representation consisting of permutation matrices on i-cells in $C_iX = C_i\overline{\mathbb{R}}$, it follows that $\iota_0 = \alpha_0$ and ι_i is equivalent to α_i up to sign for $i > 0$.

Over $\overline{\mathbb{R}^n}$ with the trivial cosheaf action, each map $\iota_i(g) : C_i\overline{\mathbb{R}^n} \to C_i\overline{\mathbb{R}^n}$ can be represented as a matrix with $\pm\mathbf{I}_n$ signed identity blocks. This is equivalent to the representation $\mathbf{I}_n \otimes \alpha_i$ on $C_i\overline{\mathbb{R}^n}$ up to sign, where $\mathbf{I}_n(g) = \mathbf{I}_n$ is the trivial representation on $\mathbb{R}^n$.

Example 3.4 (Regular representation). The group G can be considered as a discrete cell complex comprised of a point for each group element. Let (G, ℓ) be a G-cell complex where ℓ is the left action of G on itself. Suppose $(\overline{\mathbb{R}}, \iota)$ is the unit constant cosheaf over (G, ℓ) with the trivial G-action from the above example. Then the space of 0-chains $C_0(\overline{\mathbb{R}}, \iota) \cong \mathbb{R}^{|G|}$ is generated by a basis of group elements and $\iota = \iota_0 = \alpha_0$ is the *left regular representation*.

Example 3.5 (Cyclic and dihedral constant cosheaf). When G is a cyclic or dihedral group, there is a more useful representation than the trivial one over constant cosheaves. We let η be a cosheaf representation over $\overline{\mathbb{R}^2}$ determined by local maps $\eta_c(g) = [gc, c]\tau(g)$ where τ is the representation on $\mathbb{R}^2$ introduced in Example A.1. The representation $\eta_i(g)$ is equal to the representation $\tau \otimes \alpha_i$ when $i = 0$ and is equivalent up to sign when $i > 0$. See Figure 3 for an illustration.

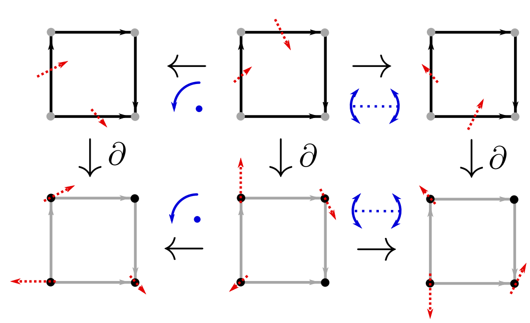

Figure 3: The D_8-constant cosheaf $(\overline{\mathbb{R}^2}, \eta_1)$ is pictured over a square cell complex, with 1- and 0-dimensional data drawn as dashed arrows (2-dimensional vectors) in edges and at vertices in the top and bottom row, respectively. Here we examine the commutativity condition (i) of Definition 3.2 over edges and vertices. To the left the group element is a $\pi/2$ rotation counter-clockwise, and to the right the group element is a reflection about the horizontal axis. Take note of the sign alignment $[ge, e] = \pm 1$ between an edge e and its permutation.

A realization $p : \mathscr{V} \to \mathbb{R}^2$ is a G-*realization* if there is a representation $\tau_0 : G \to$

$\mathrm{GL}(\mathbb{R}^2)$ over which p is equivariant. In other words, p satisfies

$$\tau_0(g)p_v = p_{gv} \tag{15}$$

for every $g \in G$ and $v \in \mathscr{V}$. We take $\tau_0 = \tau$ to be the standard representation from Example A.1. A *G-framework* is a G-cell complex (X, α) together with a G-realization forming a triple (X, α, p).

Example 3.6 (Cyclic and dihedral force cosheaf)*.* We investigate the force cosheaf $\mathcal{F}$ over such a realized G-cell complex (X, α, p). Due to the isomorphism of vertex stalks $\mathcal{F}_v \cong \overline{\mathbb{R}^2}$, we can consider the representation ρ on $\mathcal{F}$ extending the representation $\tau \otimes \alpha_0$ on $C_0\mathcal{F} \cong C_0\overline{\mathbb{R}^2}$ to 1-chains. We set $\rho_e(g) = \mathrm{id}$ between edge stalks $\mathcal{F}_e \to \mathcal{F}_{ge}$ sending a unit compression over e to unit compression over ge for every edge e and element $g \in G$. With this identification ρ_1 is equivalent to α_1, the representation of (strictly positive) permutation matrices on edge generators in $C_1\mathcal{F} \cong C_1X$. To confirm that ρ is indeed a G-representation we check the condition (12), namely the the following vectors are equal

$$\begin{aligned}[gv : ge]\mathcal{F}_{ge \triangleright gv} \circ \mathrm{id}(1) &= [gv : ge]^2(p_{gv} - p_{gu}) \\ &= [v : e]^2\tau(g)(p_v - p_u) \\ &= [v : e]\tau(g) \circ \mathcal{F}_{e \triangleright v}(1).\end{aligned}$$

Here we utilized the definitions of a G-realization (15) and of the force cosheaf extension map in line (3).

The force cosheaf $\mathcal{F}$ and its cosheaf representation ρ are used in most other sources of equivariant trusses [11, 37]. See Figure 4 for an illustration.

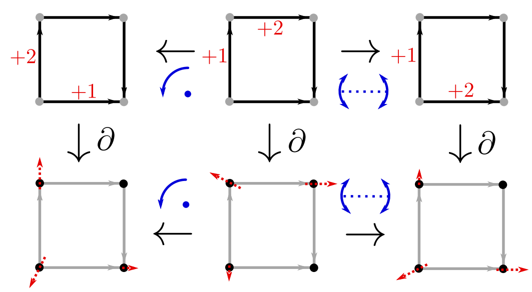

Figure 4: The D_8-force cosheaf $(\mathcal{F}, \rho)$ is pictured over a square. Data over edges are shown as scalars (top row), and data over vertices are shown as dashed arrows at vertices, as before (bottom row). Two of the edges are in varying degrees of compression, and we check condition (i) of Definition 3.2 for $\mathcal{F}$.

Let $\mu^{(1)}, \ldots, \mu^{(m)}$ denote the irreducible representations of G, unique up to isomorphism. For each dimension index i we have that $C_i\mathcal{K}$ is isomorphic to a direct sum of G-submodules

$$C_i\mathcal{K} \cong C_i^{(1)}\mathcal{K} \oplus C_i^{(2)}\mathcal{K} \oplus \cdots \oplus C_i^{(m)}\mathcal{K}$$

where $C_i^{(j)}\mathcal{K}$ is isomorphic to the direct sum of $N^{(j)}(\rho_i) \geqslant 0$ copies of the irreducible G-module $(k^{n_j}, \mu^{(j)})$. Each space $C_i^{(j)}\mathcal{K}$ has dimension $N^{(j)}(\rho_i)n_j$. (See also

Appendix A.)

Let $\partial_i^{(j)}$ denote the restriction of the boundary map ∂_i to the subspace $C_i^{(j)}\mathcal{K}$. By Theorem A.6 it follows that ∂_i can be represented by the sum

$$\partial_i = \partial_i^{(1)} \oplus \cdots \oplus \partial_i^{(m)} \tag{16}$$

over the irreducible G-submodules. The image of $\partial_i^{(j)}$ is zero on $C_{i-1}^{(t)}$ for any $t \neq j$.

Lemma 3.7. *Any G-cosheaf chain complex $C(\mathcal{K}, \rho)$ is isomorphic to the decomposition*

$$C\mathcal{K} \cong C^{(1)}\mathcal{K} \oplus \cdots \oplus C^{(m)}\mathcal{K} \tag{17}$$

where each chain complex $C^{(j)}\mathcal{K}$ is of the form

$$\cdots \to C_{i+1}^{(j)}\mathcal{K} \xrightarrow{\partial_{i+1}^{(j)}} C_i^{(j)}\mathcal{K} \xrightarrow{\partial_i^{(j)}} C_{i-1}^{(j)}\mathcal{K} \to \ldots$$

Proof. This is Theorem A.7 applied to the boundary maps ∂_i of the chain complex. □

3.1. Equivariant Cosheaf Maps

Definition 3.8 (G-cosheaf map)**.** Suppose G is a finite group, (X, α) is a G-cell complex, $(\mathcal{K}, \rho)$ and $(\mathcal{L}, \eta)$ are G-cosheaves over (X, α) and $\phi : \mathcal{K} \to \mathcal{L}$ is a cosheaf map. We say that ϕ is a *G-cosheaf map* if the diagram

$$\begin{tikzcd}
C_i\mathcal{K} \arrow[rr, "\phi"] \arrow[dr, "\rho(g)"] \arrow[dd, "\partial"'] & & C_i\mathcal{L} \arrow[dr, "\eta(g)"] \arrow[dd, "\partial"] & \\
& C_i\mathcal{K} \arrow[rr, "\phi"] \arrow[dd, "\partial"] & & C_i\mathcal{L} \arrow[dd, "\partial"] \\
C_{i-1}\mathcal{K} \arrow[rr, "\phi"] \arrow[dr, "\rho(g)"'] & & C_{i-1}\mathcal{L} \arrow[dr, "\eta(g)"] & \\
& C_{i-1}\mathcal{K} \arrow[rr, "\phi"] & & C_{i-1}\mathcal{L}
\end{tikzcd} \tag{18}$$

commutes for every index i and group element $g \in G$. This means the composition of maps over every path from $C_i\mathcal{K}$ to $C_{i-1}\mathcal{L}$ must be equal.

The commutativity of the front and back squares of diagram (18) follow from ϕ being a chain map and the commutativity of the left and right squares follow by both $\mathcal{K}$ and $\mathcal{L}$ being G-cosheaves (by assumption). The only statements that must be checked are the commutativity of the top and bottom squares of diagram (18). In particular, for every i-chain $x \in C_i\mathcal{K}$ it must be true that

$$\phi_{gc}\rho_c(g)x_c = \eta_c(g)\phi_c x_c. \tag{19}$$

Every G-cosheaf map ϕ consists of a family of G-homomorphisms on chain spaces

$\{\phi : C_i\mathcal{K} \to C_i\mathcal{L}\}$. A short exact sequence of *G-cosheaf maps*

$$0 \to C(\mathcal{K}, \rho) \xrightarrow{\phi} C(\mathcal{L}, \eta) \xrightarrow{\psi} C(\mathcal{M}, \mu) \to 0 \tag{20}$$

is a short exact sequence of cosheaf maps, equivariant under the respective representation actions. From any injective G-cosheaf map $\phi : (\mathcal{K}, \rho) \to (\mathcal{L}, \eta)$ the quotient G-cosheaf $(\mathcal{L}/\phi\mathcal{K}, \eta/\phi\rho)$ has stalks $(\mathcal{L}/\phi\mathcal{K})_c = \mathcal{L}_c/\mathrm{im}\,\phi_c\mathcal{K}_c$. The group action on stalks is the action η on quotient classes:

$$\begin{aligned}(\eta/\phi\rho)_c(g)(x + \mathrm{im}\,\phi_c) &= \eta_c(g)(x) + \mathrm{im}\,(\eta_c(g) \circ \phi_c)\\ &= \eta_c(g)(x) + \mathrm{im}\,(\phi_{gc} \circ \rho_c(g)\phi_c)\\ &= \eta_c(g)(x) + \mathrm{im}\,\phi_{gc}\end{aligned}$$

We simplify the notation by letting η/ρ denote the representation $\eta/\phi\rho$.

Example 3.9 (Cyclic and dihedral position cosheaf). Letting G be cyclic or dihedral, recall from Example 3.6 and Example 3.5 that we defined the appropriate cosheaf representations for the force $\mathcal{F}$ and constant $\overline{\mathbb{R}^2}$ cosheaves. In Example 2.6 we developed classical planar graphic statics and proved that the structure of the position cosheaf $\mathcal{P}$ can be deduced from these previous two cosheaves (without G-action). We wish to do the same *while including the G-action*, namely we show that the appropriate representation of $\mathcal{P}$ can be derived purely from the representations of $(\mathcal{F}, \rho)$ and $(\overline{\mathbb{R}^2}, \eta)$. This is the subject of Lemma 3.11, and we describe the G-cosheaf $(\mathcal{P}, \eta/\rho)$ for now.

When assuming the underlying G-cosheaf is an oriented 2-manifold, it is possible to assign every face a consistent local orientation. Then $[gf, f] = \pm 1$ depending on whether g is a rotation or a reflection. There is a simple formulation of η/ρ, namely $\eta/\rho_2 = \eta_2$ consisting of local maps

$$\eta/\rho_f(g) = \begin{cases} +\tau(g) & g \text{ is a rotation} \\ -\tau(g) & g \text{ is a reflection} \end{cases}, \tag{21}$$

which is always positive when the group G is $\mathbb{Z}_m$. Over edges the representation η/ρ_1 is similar

$$\eta/\rho_e(g) = \begin{cases} +1 & g \text{ is a rotation} \\ -1 & g \text{ is a reflection} \end{cases}. \tag{22}$$

Remark 3.10. The sign flip in Equations (21) and (22) has counter-intuitive effects. Take the reflection s (in some dihedral group) along the vertical axis; the standard representation τ takes value

$$\tau(s) = \begin{bmatrix} -1 & 0 \\ 0 & 1 \end{bmatrix} = -\begin{bmatrix} 1 & 0 \\ 0 & -1 \end{bmatrix},$$

inverting the first coordinate. Then at any face f, $\eta/\rho_f(s)$ takes the value $-\tau(s)$, which is a matrix that inverts the second coordinate, "acting like" a reflection along the horizontal axis. We can think of η/ρ having dual mirror symmetry in the dihedral group, a phenomenon previously noticed in [37]. An example of this mirror-transformation is clearly visible in Figure 1, also pictured in detail in Figure 5.

We emphasize the importance of deducing properties of the quotient G-cosheaf $(\mathcal{P}, \eta/\rho)$ purely in terms of its priors $(\mathcal{F}, \rho)$ and $(\overline{\mathbb{R}^2}, \eta)$. Universal properties (here, of quotients) are extremely powerful, and properties of any quotient G-cosheaf can be derived in an algorithmic manner by diagram chasing. The authors hope the methods used in Lemma 3.11 guide future derivations of quotient G-actions, say in Fourier methods or harmonic analysis over cosheaves.

Lemma 3.11. *The position cosheaf* $(\mathcal{P}, \eta/\rho)$ *defined in the above Example 3.9 indeed is a* $\mathbb{Z}_n$*- or* D_n*-cosheaf and* $\pi : (\overline{\mathbb{R}^2}, \eta) \to (\mathcal{P}, \eta/\rho)$ *is a* $\mathbb{Z}_n$*- or* D_n*-cosheaf map.*

Proof. Fix the group G as $\mathbb{Z}_m$ or D_{2m}. We first prove the map $\phi : \mathcal{F} \to \overline{\mathbb{R}^2}$ is in fact a G-cosheaf map satisfying the condition of line (19) at all cells and group elements. Let $(\mathcal{F}, \rho)$ and $(\overline{\mathbb{R}^2}, \eta)$ be the force and constant G-cosheaves of Examples 3.5 and 3.6. Line (19) is satisfied trivially over vertices, as both ρ_0 and η_0 are equivalent to the same representation $\tau \otimes \alpha_0$. For commutativity over edge cells, we note that $\rho_e(g) = +1$ and that $\eta_e(g) = [ge, e]\tau(g)$. Then the orientation of the edge e being preserved/reversed to ge is equivalent to the base of e (the vector $(p_u - p_v)$ for $u, v \lhd e$) being preserved/reflected, and

$$\phi_{ge} = [ge, e]\tau(g)\phi_e \tag{23}$$

Because ϕ is a G-cosheaf map, the image $\phi C\mathcal{F}$ is a G-submodule of the chain complex $C\overline{\mathbb{R}^2}$. We next prove that that quotient map π from Example 2.6 is also a well-defined G-cosheaf map, and in the process show that line (21) and line (22) hold true.

We check the commutativity of the diagram (18) for the map π over 2- and 1-chains. By assumption π is a (regular) cosheaf map, meaning the front and back squares of the diagram commute. Also the left square commutes by the construction of $(\overline{\mathbb{R}^2}, \eta)$ in Example 3.5. Clearly $\pi \circ \eta_2(g) = \eta/\rho_2(g) \circ \pi$ as maps from $C_2\overline{\mathbb{R}^2}$ to $C_2\mathcal{P}$, so the top square commutes.

We show that $\pi \circ \eta_1(g) = (\eta/\rho)_1(g) \circ \pi$, verifying the commutativity of the bottom square of diagram (18). For computations, we associate $\mathcal{P}_e$ over an edge $u, v \lhd e$ with the orthogonal space $(\phi\mathcal{F}_e)^\perp$ in $\mathbb{R}^2$ by rotating the vector $(p_u - p_v) = \phi_e(1)$ generating $\phi\mathcal{F}_e$ by angle $\pi/2$ clockwise, setting $\mathcal{P}_e \cong \operatorname{span}\{\mathbf{R}(\pi/2)\phi_e(1)\}$ where $\mathbf{R}(\cdot)$ is a rotation matrix by the specified angle. Then we define $\pi_1 : C_1\overline{\mathbb{R}^2} \to C_1\mathcal{P}$ by setting $\pi_e(y_e) = \langle \mathbf{R}(\pi/2)\phi_e(1), y_e\rangle$ for $y \in C_1\overline{\mathbb{R}^2}$. We know that at an edge e and $g \in G$, $\eta/\rho_e(g)$ is a scalar, thus we have

$$\begin{aligned}\pi_{ge} \circ \eta_e(g)(y_e) &= \eta/\rho_e \circ \pi_e(y_e) \\ [ge, e]\langle \mathbf{R}(\pi/2)\phi_{ge}(1), \tau(g)y_e\rangle &= \eta/\rho_e(g)\langle \mathbf{R}(\pi/2)\phi_e(1), y_e\rangle \\ [ge, e]^2\tau(g)^{-1}\mathbf{R}(\pi/2)\tau(g)\phi_e(1) &= \eta/\rho_e(g)\mathbf{R}(\pi/2)\phi_e(1)\end{aligned} \tag{24}$$

using line (23). This implies that

$$\eta/\rho_e(g)\phi_e(1) = \mathbf{R}(\pi/2)^{-1}\tau(g)^{-1}\mathbf{R}(\pi/2)\tau(g)\phi_e(1) = [\mathbf{R}(\pi/2), \tau(g)]\phi_e(1)$$

the commutator of the two orthogonal matrices. If g is a rotation, the matrices commute and $\eta/\rho_e = +1$. When g is a reflection then

$$\mathbf{R}(\pi/2)^{-1}\left(\tau(g)^{-1}\mathbf{R}(\pi/2)\tau(g)\right) = \mathbf{R}(\pi/2)^{-1}\mathbf{R}(\pi/2)^{-1} = \mathbf{R}(\pi)$$

sends $\phi_e(1)$ to $-\phi_e(1)$.

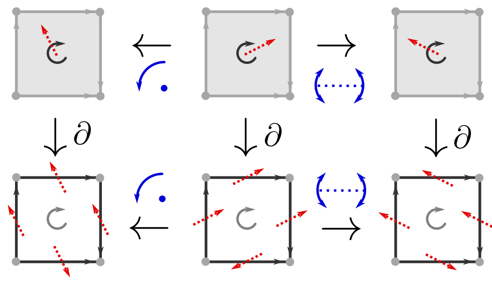

Figure 5: Generators for the representation of the D_8-constant cosheaf $(\overline{\mathbb{R}^2}, \eta_2)$ are pictured acting on a square face (two-dimensional data). The bottom row shows the 1-dimensional data (dashed vectors for the edges). This is a continuation of Figure 3. To the left, the stalks are permuted, rotated by $\pi/2$ counter-clockwise, then resigned by multiplying by the scalar $[gc, c]$. To the right, the stalks are permuted, reflected along the horizontal axis, then re-signed. The composition of reflection along the horizontal axis and negation misleadingly appears like a reflection along the vertical axis, following Remark 3.10.

For the final right commutativity square of diagram (18), we confirm that $(\mathcal{P}, \eta/\rho)$ is indeed a G-cosheaf by checking point (i) of Definition 3.2. For $x \in C_2\mathcal{P}$ the following equations are equivalent,

$$\begin{aligned} [ge : gf]\mathcal{P}_{gf \triangleright ge}\eta/\rho_f(g)x_f &= \eta/\rho_e(g)[e : f]\mathcal{P}_{f \triangleright e}x_f \\ [ge : gf][gf, f]\langle \mathbf{R}(\pi/2)\phi_{ge}(1), \tau(g)x_f\rangle &= \eta/\rho_e(g)[e : f]\langle \mathbf{R}(\pi/2)\phi_e(1), x_f\rangle, \end{aligned} \tag{25}$$

which after using equation (14), (25) is identical to line (24) swapping variables x and y. Thus π is a G-map between G-cosheaves. □

As consequence of Example 3.9 and Lemma 3.11, we know that

$$0 \to C(\mathcal{F}, \rho) \xrightarrow{\phi} C(\overline{\mathbb{R}^2}, \eta) \xrightarrow{\pi} C(\mathcal{P}, \eta/\rho) \to 0. \tag{26}$$

is an exact sequence of $\mathbb{Z}_m$- or D_{2m}-cosheaves.

4. Irreducible Representations and Homology

Previously we confirmed that cosheaves and maps between cosheaves can be enriched with group representations. From this groundwork we have the methods for separating cosheaf chains and homology cycles into their constituent irreducible components, each respecting one of the underlying symmetries of the framework.

Lemma 4.1. *To any short exact sequence of cosheaf chain complexes of the form (20), there is a short exact sequence of G-cosheaf chain complexes for each irreducible representation $\mu^{(j)}$ of G:*

$$0 \to C^{(j)}(\mathcal{K}, \rho) \xrightarrow{\phi^{(j)}} C^{(j)}(\mathcal{L}, \eta) \xrightarrow{\psi^{(j)}} C^{(j)}(\mathcal{L}/\mathcal{K}, \eta/\rho) \to 0 \tag{27}$$

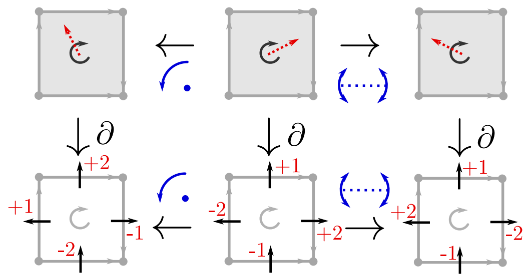

Figure 6: Generators for the representation of the position cosheaf $(\mathcal{P}, \eta/\rho)$ are pictured acting on a square face. Note that the top row is identical to that of Figure 5, and the basis vectors orthogonal to edges are drawn in the bottom row. The vector in the top-center square has components $(+2, +1)$ in the x and y directions. To the left, vectors/scalars are permuted and rotated by $\pi/2$ counter-clockwise. To the right, the square is reflected along the horizontal axis, then some vectors/scalars reverse sign following Equation (21). The composition appears like a reflection along the vertical axis, following Remark 3.10.

Proof. Each component chain map $\phi_i : C_i\mathcal{K} \to C_i\mathcal{L}$ and $\psi_i : C_i\mathcal{L} \to C_i\mathcal{M}$ are G-homomorphisms. By Theorem A.7 the sequence

$$0 \to C_i^{(j)}(\mathcal{K}, \rho) \xrightarrow{\phi_i^{(j)}} C_i^{(j)}(\mathcal{L}, \eta) \xrightarrow{\psi_i^{(j)}} C_i^{(j)}(\mathcal{L}/\mathcal{K}, \eta/\rho) \to 0 \tag{28}$$

of i-chains is exact. We know ϕ_i and ψ_i commute with the respective cosheaf boundary maps ∂ which likewise decompose along the irreducible components in line (16). Thus exact sequences of G-modules (28) extend to exact sequences of G-chain complexes (27). ∎

The long exact sequence (9) respects the group action of the G-cosheaves. We have seen that representations $\rho(g) : C\mathcal{K} \to C\mathcal{K}$ and $\eta(g) : C\mathcal{L} \to C\mathcal{L}$ are chain complex automorphisms for each $g \in G$. These maps (as quasi-automorphisms) induce isomorphisms in homology $\rho(g) : H\mathcal{K} \to H\mathcal{K}$ and $\eta : H\mathcal{L} \to H\mathcal{L}$. The following diagram with exact rows commutes for every $g \in G$:

$$\begin{tikzcd}
\dots \arrow[r, "\psi"] & H_{i+1}\mathcal{L}/\mathcal{K} \arrow[r, "\vartheta"] \arrow[d, "\eta/\rho(g)"] & H_i\mathcal{K} \arrow[r, "\phi"] \arrow[d, "\rho(g)"] & H_i\mathcal{L} \arrow[r, "\psi"] \arrow[d, "\eta(g)"] & H_i\mathcal{L}/\mathcal{K} \arrow[r, "\vartheta"] \arrow[d, "\eta/\rho(g)"] & \dots \\
\dots \arrow[r, "\psi"] & H_{i+1}\mathcal{L}/\mathcal{K} \arrow[r, "\vartheta"] & H_i\mathcal{K} \arrow[r, "\phi"] & H_i\mathcal{L} \arrow[r, "\psi"] & H_i\mathcal{L}/\mathcal{K} \arrow[r, "\vartheta"] & \dots
\end{tikzcd} \tag{29}$$

following from the naturality of the long exact sequence [26].

Lemma 4.2. *Every long exact sequence of G-cosheaf homology splits into irreducible factors. For a short exact sequence of G-cosheaves, to each irreducible representation*

$\mu^{(j)}$ of G the sequence

$$\cdots \to H_{i+1}^{(j)}\mathcal{L}/\mathcal{K} \xrightarrow{\vartheta^{(j)}} H_i^{(j)}\mathcal{K} \xrightarrow{\phi^{(j)}} H_i^{(j)}\mathcal{L} \xrightarrow{\psi^{(j)}} H_i^{(j)}\mathcal{L}/\mathcal{K} \to \dots \tag{30}$$

is exact.

Proof. Line (30) is the long exact sequence of the chain complex (27). By Theorem A.7, the connecting homomorphism $\vartheta^{(j)}$ is exactly the (j)-th irreducible component of the full connecting G-homomorphism $\vartheta : H_{i+1}\mathcal{L}/\mathcal{K} \to H_i\mathcal{K}$ from diagram (29). □

4.1. A Symmetrical Maxwell Counting Rule

Characters have useful orthogonality and projection properties [29] that make character theory a critical tool for counting the dimensions of chain and homology spaces (see also Appendix A.) We demonstrate the utility of character theory by formulating a symmetric version of Maxwell's rule for frameworks in terms of a symmetric Euler characteristic for chain complexes using characters.

The *Euler characteristic* of a finite dimensional chain complex C is the alternating sum of the dimensions

$$\mathcal{X}(C) = \sum_i (-1)^i \dim C_i$$

The Euler formula has found use in molecular chemistry [7], DNA polyhedra [28], configuration spaces in robotics [18], and of course in structural mechanics [11, 12] among many other applications.

Theorem 4.3 (Standard Euler Characteristic [26])**.** *The Euler characteristic of a finite dimensional chain complex and its homology are equal. In particular, for a cosheaf $\mathcal{K}$ with finite dimensional stalks over a finite dimensional cell complex we have*

$$\mathcal{X}(C\mathcal{F}) = \sum_i (-1)^i \dim C_i\mathcal{K} = \sum_i (-1)^i \dim H_i\mathcal{K} = \mathcal{X}(H\mathcal{F}).$$

Theorem 4.3 also applies to chain complexes corresponding to the irreducible representations of G, namely $\mathcal{X}(C^{(j)}\mathcal{K}) = \mathcal{X}(H^{(j)}\mathcal{K})$.

The well-known *Maxwell counting rule* is the statement that the difference in dimensions of self stresses and kinematic degrees of freedom is equivalent to counting the different dimension cells of a finite framework [6]; in two dimensions this is the equation

$$\#\text{kinematic degrees of freedom} - \#\text{self stress dimensions} = 2\#\text{vertices} - \#\text{edges} \tag{31}$$

where global translation and rotation assignments are included in the kinematic space. This is exactly the application of Theorem 4.3 to the force cosheaf $\mathcal{F}$ [12].

Over a G-framework (X, α, p), the Maxwell counting rule (31) takes a more refined form. At the identity element ϵ, the character $\chi_\rho(\epsilon) = \text{trace}(\rho(\epsilon))$ is nothing more than the degree of χ_ρ. Therefore the Standard Euler Characteristic Theorem (Theorem 4.3) for a G-cosheaf $(\mathcal{K}, \rho)$ can be reformulated as

$$\mathcal{X}(C\mathcal{K}) = \sum_i (-1)^i \chi(\rho_i)(\epsilon) = \sum_i (-1)^i \chi(\rho_{H_i\mathcal{K}})(\epsilon) = \mathcal{X}(H\mathcal{K}). \tag{32}$$

However, there is no need to restrict the character $\chi(\rho)$ to only the identity element. Equation (32) in vector form (in $\mathbb{C}^{|G|}$) is

$$\sum_i (-1)^i \chi(\rho_i) = \sum_i (-1)^i \chi(\rho_{H_i\mathcal{K}}), \tag{33}$$

which is quickly seen from repeated application of Theorem A.4 and character identities (45). Equation (33) applies to any G-cosheaf chain complex $(C\mathcal{K}, \rho)$, including its irreducible component chain complexes $(C^{(j)}\mathcal{K}, \rho)$. For any index (j) the following identity holds:

$$\sum_i (-1)^i \chi(\rho_i^{(j)}) = \sum_i (-1)^i \chi(\rho_{H_i\mathcal{K}}^{(j)}). \tag{34}$$

Definition 4.4. For a finite group G, the *symmetric Euler characteristic* of a finite dimensional G-chain complex (C, ρ) is

$$\hat{\mathcal{X}}(C, \rho) = \left(\sum_i (-1)^i N^{(1)}(\rho_i), \ldots, \sum_i (-1)^i N^{(m)}(\rho_i) \right), \tag{35}$$

an m-tuple of integers where m is the number of irreducible representations of the group G, and $N^{(j)}(\rho_i)$ is defined in Appendix A (see Theorem A.9).

Theorem 4.5 (Symmetric Euler characteristic)**.** *For a finite group G, the symmetric Euler chararacteristics of a finite G-chain complex and its homology are equal. In particular for a G-cosheaf $\mathcal{K}$ with finite dimensional stalks over a finite dimensional cell complex, the (j)-th components of the symmetric Euler characteristics are equal to*

$$\hat{\mathcal{X}}^{(j)}(C\mathcal{K}, \rho) = \sum_i (-1)^i N^{(j)}(\rho_i) = \sum_i (-1)^i N^{(j)}(\rho_{H_i\mathcal{K}}) = \hat{\mathcal{X}}^{(j)}(H\mathcal{K}, \rho_{H\mathcal{K}}) \tag{36}$$

for every index (j).

Proof. Clearly the equalities

$$\hat{\mathcal{X}}^{(j)}(C\mathcal{K}, \rho) \cdot \chi(\mu^{(j)}) = \sum_i (-1)^i N^{(j)}(\rho_i) \cdot \chi(\mu^{(j)}) = \sum_i (-1)^i \chi(\rho_i^{(j)})$$

hold by the defining Equation (35). A similar equality holds for homologies $\hat{\mathcal{X}}^{(j)}(H\mathcal{K}, \rho_{H\mathcal{K}})$. The result then follows from Equation (34). □

Note that when G is the trivial group, the extended Euler characteristic $\hat{\mathcal{X}}(C\mathcal{K}, \mathrm{id})$ is nothing more than the standard Euler characteristic $\mathcal{X}(C\mathcal{K})$. In fact, for any finite group the standard Euler characteristic can be recovered by taking the degree of both sides of Equation (49); this is the weighted sum

$$\mathcal{X}(C\mathcal{K}) = \sum_i (-1)^i \deg \chi(\rho_i) = \sum_i \sum_{(j)} (-1)^i N^{(j)}(\rho_i) \cdot \deg \chi(\mu^{(j)}) = \sum_{(j)} \hat{\mathcal{X}}^{(j)}(C\mathcal{K}, \rho) \cdot \dim \mu^{(j)}.$$

Over the G-force cosheaf $(\mathcal{F}, \rho)$, Equation (36) is the *symmetric Maxwell rule*, the analogue of Equation (31) in the group equivariant setting. While the standard

Euler characteristic $\mathcal{X}(C\mathcal{F})$ is an alternating sum of numbers of cells by dimension, the components of $\hat{\mathcal{X}}(C\mathcal{F})$ are alternating sums of *symmetric force chains* detailed in numerous previous works [19, 10, 11]. The symmetric Maxwell rule is useful for quickly detecting self-stresses of different symmetry types, which are undetectable using standard non-symmetric counts.

Example 4.6. To demonstrate the symmetric Maxwell rule we re-examine the mirror-symmetric framework in Figure 1(a). For this example, we have $2\#\text{vertices} - \#\text{edges} = 12 - 9 = 3$ and hence the standard Maxwell rule given in Equation (31) only detects the three trivial degrees of freedom in the plane and no self-stress. However, using Theorem 4.5 we can detect the self-stress indicated in Figure 1(a).

Aligned with the trivial representation $\mu^{(1)}$, the chain complex $C^{(1)}\mathcal{F}$ consists of chains that are fixed by every group action on the underlying space. The space $C_0^{(1)}\mathcal{F}$ is spanned by fully mirror-symmetric vector assignments to vertices; these are spanned by vertical forces assignments to nodes B and C, as well as mirror-symmetric force pairs to A-C and D-F causing $N^{(1)}(\rho_0) = 2 + 2 \cdot 2 = 6$. The space $C_1^{(1)}\mathcal{F}$ is spanned by symmetric edge-assignments, the dimension of which (for the force cosheaf $\mathcal{F}$) is equivalent to the number of edge orbits. Because three edges lie along the axis of symmetry and six don't, $N^{(1)}(\rho_1) = 3 + 6/2 = 6$.

The symmetric Maxwell rule states that for the trivial index (1), the equation

$$\hat{\mathcal{X}}^{(1)}(C\mathcal{F}, \rho) = \hat{\mathcal{X}}^{(1)}(H\mathcal{F}, \rho_{H\mathcal{F}})$$

evaluates to the following equation

$$N^{(1)}(\rho_0) - N^{(1)}(\rho_1) = 6 - 6 = 0 = N^{(1)}(\rho_{H_0\mathcal{F}}) - N^{(1)}(\rho_{H_1\mathcal{F}}) = \dim H_0^{(1)}\mathcal{F} - \dim H_1^{(1)}\mathcal{F}$$

using $\dim \mu^{(1)} = 1$. This means that there is an equal number of mirror symmetric self-stresses as kinematic degrees of freedom. But the vertical translation of the framework along the mirror line is clearly mirror-symmetric and hence we conclude that there must also be a mirror-symmetric self-stress (as indicated in Figure 1(a)).

In general, the symmetry-extended Maxwell rule often provides significantly more insights into self-stresses and infinitesimal motions of frameworks than the standard Maxwell counts (see also e.g. [19, 10, 11]). As such, it has become a powerful tool in geometric rigidity theory and its applications. Recently, it has also been used as a design tool for engineering structures with self-stresses of desired symmetry types (see e.g. [38, 35]).

4.2. Symmetric Graphic Statics

We recall that the exact sequence of G-chain complexes (26) is isomorphic to a direct sum of irreducible chain complex components of the form (17). For a given irreducible representation of G with index (j), the following diagram commutes with exact rows

$$\begin{tikzcd}
 & 0 \arrow[r] \arrow[d] & C_2^{(j)}\overline{\mathbb{R}^2} \arrow[r, "\pi^{(j)}"] \arrow[d, "\partial^{(j)}"] & C_2^{(j)}\mathcal{P} \arrow[r] \arrow[d, "\partial^{(j)}"] & 0 \\
0 \arrow[r] & C_1^{(j)}\mathcal{F} \arrow[r, "\phi^{(j)}"] \arrow[d, "\partial^{(j)}"] & C_1^{(j)}\overline{\mathbb{R}^2} \arrow[r, "\pi^{(j)}"] \arrow[d, "\partial^{(j)}"] & C_1^{(j)}\mathcal{P} \arrow[r] \arrow[d] & 0 \\
0 \arrow[r] & C_0^{(j)}\mathcal{F} \arrow[r, "\phi^{(j)}"] & C_0^{(j)}\overline{\mathbb{R}^2} \arrow[r] & 0 &
\end{tikzcd}$$

summarizing the relationship between the symmetric chains (force loadings and positions) relevant in graphic statics.

Because $H_1X = 0$ and thus $H_1\overline{\mathbb{R}^2} = 0$, it follows that $H_1^{(j)}\overline{\mathbb{R}^2} = 0$ for each (j). The homology spaces $H_2\overline{\mathbb{R}^2}$ and $H_0\overline{\mathbb{R}^2}$ consist of constant vector assignments to every face and vertex in X. Consequently, the G-modules $(H_i\overline{\mathbb{R}^2}, \eta_{H_i\overline{\mathbb{R}^2}})$ and $(\mathbb{R}^2, \tau)$ are equivalent for $i = 0, 2$ and the isomorphism $\mathbb{R}^2 \to H_i\overline{\mathbb{R}^2}$ is the diagonal map.

Utilizing Lemma 4.2, the long exact sequence corresponding to an irreducible representation $\mu^{(j)}$ splits into two exact sequences

$$0 \to H_2^{(j)}\overline{\mathbb{R}^2} \xrightarrow{\pi^{(j)}} H_2^{(j)}\mathcal{P} \xrightarrow{\vartheta^{(j)}} H_1^{(j)}\mathcal{F} \to 0 \tag{37}$$

$$0 \to H_1^{(j)}\mathcal{P} \xrightarrow{\vartheta^{(j)}} H_0^{(j)}\mathcal{F} \xrightarrow{\phi^{(j)}} H_0^{(j)}\overline{\mathbb{R}^2} \to 0,$$

where the former exact sequence describes the $\mu^{(j)}$-symmetric components of the graphic statics relation, described previously in Example 2.6.

Theorem 4.7 (Symmetric planar 2D graphic statics)**.** *Let (X, α, p) be a planar G-framework in $\mathbb{R}^2$. For each irreducible representation $\mu^{(j)}$ of G, there is an isomorphism between $\mu^{(j)}$-symmetric self-stresses and $\mu^{(j)}$-symmetric realizations of the dual G-cell complex up to $\mu^{(j)}$-translational symmetry.*

Proof. The first exact sequence (37) reduces to

$$0 \to (\mathbb{R}^2)^{(j)} \xrightarrow{\pi^{(j)}} H_2^{(j)}\mathcal{P} \xrightarrow{\vartheta^{(j)}} H_1^{(j)}\mathcal{F} \to 0 \tag{38}$$

meaning $\vartheta^{(j)} : H_2^{(j)}\mathcal{P}/\pi^{(j)}(\mathbb{R}^2)^{(j)} \cong H_1^{(j)}\mathcal{F}$ is an isomorphism. The image $\pi^{(j)}(\mathbb{R}^2)^{(j)}$ consists of the $\tau^{(j)}$-constant vector assignments to all faces of X (constant translational assignments to dual vertices). □

Theorem 4.7 is a key result in the development of symmetric graphic statics, significantly extending the work in [37], which only considers reciprocal diagrams arising from "fully-symmetric" self-stresses. It proves and provides the algebraic maps needed to relate self-stresses of different symmetry types in primal frameworks with their dual frameworks while maneuvering past formerly perplexing issues (see Remark 3.10). The components of homology spaces associated to each symmetry type may be analyzed independently, paring down computational burden. This formalization of graphic statics relationships may also aid symmetric kinematic analysis [35, 37].

Example 4.8. A truss with one degree of self-stress and D_2 (mirror) symmetry is pictured in Figure 1(a). Its three degrees of reciprocal diagrams are either $\mu^{(1)}$- or $\mu^{(2)}$-symmetric, which we now describe.

The group D_2 has two irreducible one-dimensional representations, the trivial representation $\mu^{(1)}$ and the representation $\mu^{(2)}$ that takes value -1 on the reflection $s \in D_2$. The self-stress pictured in Figure 1(a) corresponds to the former, with $H_1^{(1)}\mathcal{F} = H_1\mathcal{F}$ having dimension 1. The representation $\tau^{(1)}$ is one-dimensional, and the graphic statics sequence (38) with superscript (1) has isomorphic entries to

$$0 \to \mathbb{R} \to H_2^{(1)}\mathcal{P} \xrightarrow{\vartheta^{(1)}} H_1^{(1)}\mathcal{F} \to 0$$

Here $H_2^{(1)}\overline{\mathbb{R}^2} \cong \mathbb{R}$ consists of the left-right translations of the reciprocal (b). One dimension of $H_2^{(1)}\mathcal{P}$ corresponds to this horizontal translation, while the other scales the diagram pictured in (b) corresponding to the self-stress in (a). The exact sequence (38) for superscript (2) is equivalent to

$$0 \to \mathbb{R} \to H_2^{(2)}\mathcal{P} \to 0$$

where $H_2^{(2)}\overline{\mathbb{R}^2} \cong \mathbb{R}$ consists of the up-down translations of the reciprocal, which are inverted by the action $\eta_f(s) = -\tau(s)$ over the reflection s at every face/dual vertex.

It is a standard method in representation theory to split the homology space $H_2\mathcal{P}$ into its components $H_2^{(1)}\mathcal{P}$ and $H_2^{(2)}\mathcal{P}$ in computations. For each irreducible representation $\mu^{(j)}$, we form the linear map

$$\gamma^{(j)} := \sum_{g \in G} \chi(\mu^{(j)})(g) \cdot \eta/\rho(g) : C_2\mathcal{P} \to C_2\mathcal{P}. \tag{39}$$

Then $\gamma^{(j)}$ has image $C_2^{(j)}\mathcal{P}$, and when restricted to homology cycles the map $\gamma^{(j)}|_{H_2\mathcal{P}}$ has the desired image $H_2^{(j)}\mathcal{P}$. This method (39) will also be used in the example in Appendix B.

5. Conclusion and Future Work

We have developed graphic statics for symmetric frameworks, decomposing the classical self-stress to reciprocal diagram correspondence by the irreducible representations of the finite group. These reciprocal diagrams are useful as both a geometric visualization of the internal stresses and as a design tool for the framework (and its polyhedral liftings). Through the symmetric graphic statics result – Theorem 4.7 – frameworks can now be designed graphically along the symmetry of their internal stresses. A detailed example is provided in Appendix B. (See also Example 4.8 and the example shown in Figure 7.)

It is straightforward to generalize the methods here to frameworks with exterior loadings as well as polyhedral lifts of self-stressed frameworks with cyclic and dihedral symmetry. This leads to the natural question of formulating equivariant cosheaves over *periodic* stressed frameworks, considered as the lift of a toroidal lifting [17] to the simply connected cover $\mathbb{R}^2$. The group characters and representations are then intimately related to the discrete Fourier transform by the Peter-Weyl theorem, indicating a deep connection with methods in harmonic analysis [32]. In higher

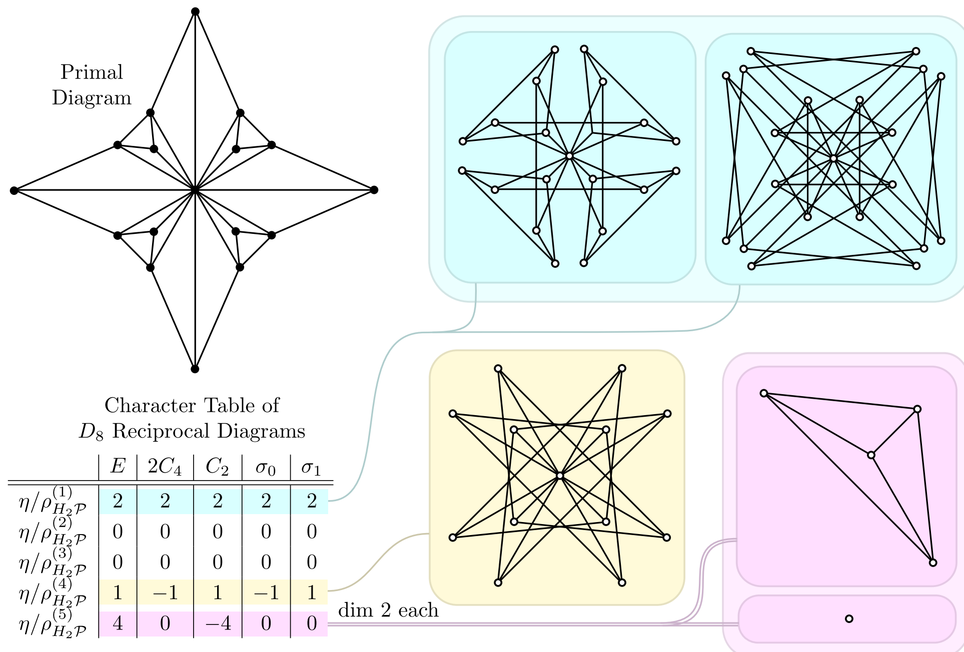

	E	$2C_4$	C_2	σ_0	σ_1
$\eta/\rho^{(1)}_{H_2\mathcal{P}}$	2	2	2	2	2
$\eta/\rho^{(2)}_{H_2\mathcal{P}}$	0	0	0	0	0
$\eta/\rho^{(3)}_{H_2\mathcal{P}}$	0	0	0	0	0
$\eta/\rho^{(4)}_{H_2\mathcal{P}}$	1	-1	1	-1	1
$\eta/\rho^{(5)}_{H_2\mathcal{P}}$	4	0	-4	0	0

Figure 7: A framework with D_8 dihedral symmetry and a family of reciprocal frameworks corresponding to irreducible representations of D_8. The last irreducible representation $\mu^{(5)}$ has dimension two. Then, with the space $H_2^{(5)}\mathcal{P}$ being 4-dimensional the representation $\eta/\rho^{(5)}_{H_2\mathcal{P}}$ consists of two factors of $\mu^{(5)}$. The result is that the four dimensions of reciprocal diagrams are grouped into pairs of two each. Note that point coordinates may overlap in the reciprocal frameworks, and in such cases, nodes and edges might not be visible in the drawing.

dimensions, there are potential extensions of this work to vector graphic statics [1], 3D-graphic statics [22], and beyond.

The kinematics and dynamics of symmetric structures can likewise be investigated homologically and equivariantly. The instantaneous velocities of a framework (treated as a pinned linkage) are homology classes [13] and could be treated with the cosheaf method. This may be particularly useful for modeling the folding of symmetric origami, which have found remarkable applications in deployable aerospace structures, biomedical devices, and metamaterials [31]. We note that after applying such a velocity for some finite time, the underlying framework symmetry may change.

It is open to study the actions of subgroups $H \leqslant G$ and the relations between representations and characters under subgroup restriction or Brauer induction, such as the approach in [4]. We suspect one can define a sheaf theoretic analogue of Bredon homology [34]; however this would require extra structure outside of the scope of this paper. Moreover, it is unclear how to interpret equivariant homology groups of a cosheaf, but we believe that it is worthy of further investigation.

There has been much previous work on the *quotient framework* of a symmetric framework (with possible self-loops) under the group action in question [40, 37]. One consequence of this work is that the self-stresses of quotient frameworks are identified as an *equivariant homology* space. It is well known that when G is a free action, a G-sheaf on X is equivalent to an ordinary sheaf on X/G [3]. We suspect that methods from equivariant homology theory [30] can be utilized towards the understanding of quotient frameworks and structures.

Acknowledgements

Bernd Schulze was partially supported by the ICMS Knowledge Exchange Catalyst Programme. Zoe Cooperband and Miguel Lopez were supported by the Air Force Office of Scientific Research under award number FA9550-21-1-0334 while at the University of Pennsylvania. The authors are grateful for their illuminating discussions with Robert Ghrist, Jakob Hansen, Maxine Calle, and Mona Merling.

References

[1] D'Acunto et al. "Vector-Based 3D Graphic Statics: A Framework for the Design of Spatial Structures Based on the Relation between Form and Forces". *Int. J. Solids Struct.* 167 (2019), pp. 58–70.

[2] P. W. Atkins, M. S. Child, and C. S. G. Phillips. *Tables for Group Theory.* Oxford University Press, 1970.

[3] J. Bernstein and V. Lunts. *Equivariant sheaves and functors.* Lecture notes in mathematics. Springer-Verlag Berlin Heidelberg, 1994.

[4] R. Boltje. "Identities in representation theory via chain complexes". *J. Algebra* 167.2 (1994), pp. 417–447.

[5] M. M. Bronstein, J. Bruna, T. Cohen, and P. Veličković. "Geometric deep learning: Grids, groups, graphs, geodesics, and gauges". *arXiv:2104.13478* (2021).

[6] C. R. Calladine. "Buckminster Fuller's Tensegrity Structures and Clerk Maxwell's Rules for the Construction of Stiff Frames". *Int. J. Solids Struct.* 14.2 (1978), pp. 161–172.

[7] A. Ceulemans and P. W. Fowler. "Extension of Euler's theorem to symmetry properties of polyhedra". *Nature* 353.6339 (1991), pp. 52–54.

[8] T. Cohen and M. Welling. "Group equivariant convolutional networks". *Int. conf. on machine learning.* PMLR. 2016, pp. 2990–2999.

[9] R. Connelly, E. Demaine, and G. Rote. "Straightening polygonal arcs and convexifying polygonal cycles". *Discrete Comput. Geom.* 30.2 (2003), pp. 205–239.

[10] R. Connelly, P.W. Fowler, S.D. Guest, B. Schulze, and W.J. Whiteley. "When is a symmetric pin-jointed framework isostatic?" *Int. J. Solids Struct.* 46.3 (2009), pp. 762–773.

[11] R. Connelly and S. D. Guest. *Frameworks, Tensegrities, and Symmetry.* Cambridge University Press, 2022.

[12] Z. Cooperband and R. Ghrist. "Towards Homological Methods in Graphic Statics". *Proc. IASS* (2023).

[13] Z. Cooperband, R. Ghrist, and J. Hansen. "A Cosheaf Theory of Reciprocal Figures: Planar and Higher Genus Graphic Statics". *arXiv:2311.12946* (2023).
[14] H. Crapo and W. Whiteley. "Autocontraintes planes et polyèdres projetés. I. Le motif de base". *Struct. Top.* 20 (1993). Dual French-English text, pp. 55–78.
[15] L. Cremona. *Le figure reciproche nella statica grafica del prof. L. Cremona.* Tipografia di Giuseppe Bernardoni, 1872.
[16] J. Curry. "Sheaves, Cosheaves and Applications". *arXiv:1303.3255* (2014).
[17] J. Erickson and P. Lin. "A toroidal Maxwell-Cremona-Delaunay correspondence". *J. Comput. Geom.* 12.2 (2021), pp. 55–85.
[18] M. Farber. *Invitation to topological robotics.* Vol. 8. Eur. Math. Soc., 2008.
[19] P. W. Fowler and S.D. Guest. "A symmetry extension of Maxwell's rule for rigidity of frames". *Int. J. Solids Struct.* 37.12 (2000), pp. 1793–1804.
[20] R. Ghrist and Y. Hiraoka. "Network Codings and Sheaf Cohomology". *IEICE Proc. Series.* Vol. 45. Kobe, Japan: NOLTA2011, 2011, pp. 266–269.
[21] M. Hablicsek and M. Akbarzadeh. "Structural form-finding of Auxetic Materials using Graphic Statics". *Proc. IASS* (2021), pp. 1–11.
[22] M. Hablicsek, M. Akbarzadeh, and Y. Guo. "Algebraic 3D Graphic Statics: Reciprocal Constructions". *Comput. Aided Des.* 108 (2019), pp. 30–41.
[23] J. Hansen and R. Ghrist. "Distributed Optimization with Sheaf Homological Constraints". *57th Annual Allerton Conf. on Communication, Control, and Computing.* IEEE. 2019, pp. 565–571.
[24] J. Hansen and R. Ghrist. "Opinion Dynamics on Discourse Sheaves". *SIAM J. Applied Math.* 81.5 (2021), pp. 2033–2060.
[25] J. Hansen and R. Ghrist. "Toward a Spectral Theory of Cellular Sheaves". *J. Appl. Comput. Topol.* 3.4 (2019), pp. 315–358.
[26] A. Hatcher. *Algebraic Topology.* Cambridge University Press, 2002.
[27] J. E. Hopcroft and P. J. Kahn. "A paradigm for robust geometric algorithms". *Algorithmica* 7.1-6 (1992), pp. 339–380.
[28] G. Hu, W.-Y. Qiu, and A. Ceulemans. "A new Euler's formula for DNA polyhedra". *PLoS One* 6.10 (2011), e26308.
[29] G. James and M. Liebeck. *Representations and Characters of Groups.* Cambridge University Press, 1993.
[30] J.D.S. Jones. "Cyclic homology and equivariant homology". *Invent. Math.* 87.2 (1987), pp. 403–423.
[31] L. Lu, S. Leanza, and R. R. Zhao. "Origami with rotational symmetry: A review on their mechanics and design". *Appl. Mech. Rev.* 75.5 (2023), p. 050801.
[32] G. W. Mackey. "Harmonic analysis as the exploitation of symmetry-a historical survey". *Bull. Am. Math. Soc.* 3.1 (1980), pp. 543–698.
[33] J. C. Maxwell. "On reciprocal figures and diagrams of forces". *London, Edinburgh, and Dublin Phil. Mag J. Sci* 27.182 (1864), pp. 250–261.
[34] P. May. *Equivariant Homotopy and Cohomology Theory.* Vol. 91. CBMS Regional Conference Series in Mathematics. American Mathematical Society, 1996.
[35] C. Millar, B. Schulze, A. Mazurek, and W. Baker. "Symmetry and the design of self-stressed structures". *Int. J. Space Struct.* 38.4 (2023), pp. 247–261.
[36] N. A. Nguyen, M. Gulan, S. Olaru, and P. Rodriguez-Ayerbe. "Convex lifting: Theory and control applications". *IEEE Trans. Autom. Control* 63.5 (2017), pp. 1243–1258.

[37] B. Schulze and C. Millar. "Graphic statics and symmetry". *Int. J. Solids Struct.* 283 (2023), p. 112492.
[38] B. Schulze, C. Millar, A. Mazurek, and W. Baker. "States of self-stress in symmetric frameworks and applications". *Int. J. Solids Struct.* 234–235 (2022), p. 111238.
[39] B. Schulze and S. Tanigawa. "Infinitesimal rigidity of symmetric bar-joint frameworks". *SIAM J. Discr. Math.* 29.3 (2015), pp. 1259–1286.
[40] B. Schulze and W. Whiteley. "Rigidity of symmetric frameworks". *Handbook of Discrete and Computational Geometry, Third Edition.* C.D. Toth, J. O'Rourke, J.E. Goodman, editors. Chapman & Hall CRC, 2018.
[41] A. D. Shepard. "A Cellular Description of the Derived Category of a Stratified Space". *PhD thesis, Brown University* (1986).
[42] R. Short, J. Cleveland, Z. Cooperband, and M. Moy. "On the Current State of Sheaf Theoretic Networking". *2022 IEEE Int. Conf. Wirel. Space Extreme Environ (WiSEE).* Institute of Electrical and Electronics Engineers. 2022.
[43] I. Streinu. "Erratum to Pseudo-triangulations, rigidity and motion planning". *Discrete Comput. Geom.* 35.2 (2006), p. 558.
[44] W. Whiteley. "Motions and stresses of projected polyhedra". *Struct. Top.* 7 (1982). With a French translation, pp. 13–38.

Appendix A. Finite Group Representations

We review the necessary definitions and results from group representation theory. A *group representation* is a homomorphism $\rho : G \to \mathrm{GL}_k(W)$ where G is a group and W is a vector space over some field k. In this paper we require the field k to be $\mathbb{R}$ or $\mathbb{C}$ and the group G to be finite. The dimension of W is said to be the *dimension* of ρ. We say (W, ρ) is a $(k)G$*-module* under the group action $g \cdot w := \rho(g)w$ transforming vectors $w \in W$. If ρ is clear from the context, then we also just write W for (W, ρ).

Example A.1 (Standard representation of cyclic and dihedral groups). Let $\mathbb{Z}_m$ denote the cyclic group on m elements and D_{2m} denote the dihedral group of order $2m$. (Note that $\mathbb{Z}_2 = D_2$.) These groups act on the plane $\mathbb{R}^2$ by rotations and reflections by a two-dimensional *standard representation* τ. Picking a rotation generator r_1, $\tau(r_1) \in SO(2)$ is a rotation matrix by angle $2\pi/m$. For a reflection s, $\tau(s)$ is a determinant -1 matrix with eigenvectors parallel or perpendicular to the line of reflection.

We say two representations ρ_0 and ρ_1 are *equivalent* if there exists an invertable matrix $\mathbf{P}$ such that

$$\rho_0 = \mathbf{P}^{-1}\rho_1\mathbf{P} \tag{40}$$

where we regard $\mathbf{P}$ as a change in basis. In coordinates, if $\mathscr{B}_0$ is a set of basis vectors for V_0 and $\mathscr{B}_1$ is a basis for V_1, then there is an invertable matrix $\mathbf{P}$ such that for each basis vector $b_0 \in \mathscr{B}_0$ and $b_1 \in \mathscr{B}_1$, $b_1 = \mathbf{P}b_0$.

Suppose that (V, ρ) and (W, η) are G-modules. A G*-homomorphism* $\phi : (V, \rho) \to (W, \eta)$ is a linear map $\phi : V \to W$ satisfying the natural equality $\eta(g) \circ \phi = \phi \circ \rho(g)$ for every $g \in G$. We say that (V, ρ) and (W, η) are isomorphic G-modules if there exists a G-isomorphism between them.

Suppose W is a subspace of a G-module (V, ρ). We say that W is a (ρ-invariant) G-*submodule* if $\rho(g)w \in W$ for every $w \in W$. Then ρ induces a representation $\rho_W : G \to \mathrm{GL}_k(W)$ consisting of the restriction of ρ to the subspace. The resulting embedding $(W, \rho_W) \to (V, \rho)$ is a G-homomorphism.

If (W, ρ_W) is a G-submodule of (V, ρ) we construct the G-quotient space $(V/W, \rho/\rho_W)$. The group G acts on a quotient vector $x + W$ by

$$\rho/\rho_W(g)(x + W) = \rho(g)(x) + \rho(g)W = \rho(g)(x) + W. \tag{41}$$

Because the field k is $\mathbb{R}$ or $\mathbb{C}$, by Maschke's Theorem there is a G-submodule (U, η) such that (V, ρ) is isomorphic to $(W \oplus U, \rho_W \oplus \eta)$ [29].

A G-module (V, ρ) is *irreducible* (and ρ is irreducible) if its only G-submodules are zero and (V, ρ) itself. If (W_0, ρ_1) and (W_1, ρ_2) are G-submodules of V such that $V \cong W_0 \oplus W_1$, then the representation ρ is equivalent to the direct sum

$$(\rho_0 \oplus \rho_1)(g) = \begin{bmatrix} \rho_0(g) & 0 \\ 0 & \rho_1(g) \end{bmatrix}_{\mathscr{B}_0 \cup \mathscr{B}_1}$$

in the basis $\mathscr{B}_0 \cup \mathscr{B}_1$ of $W_0 \oplus W_1$, the ordered union of basis sets $\mathscr{B}_0$ for W_0 and $\mathscr{B}_1$ for W_1. Clearly the representations (V, ρ) and $(W_0 \oplus W_1, \rho_0 \oplus \rho_1)$ are isomorphic.

Example A.2 (Irreducible representations of common groups). The group $\mathbb{Z}_2$ has two 1-dimensional irreducible representations, namely the one that assigns 1 to both group elements, denoted by $\mu^{(1)}$, and the one that assigns 1 to the trivial and -1 to the non-trivial group element, denoted by $\mu^{(2)}$. It is easy to see that the standard representation τ over $\mathbb{Z}_2$ from Example A.1 decomposes as $\tau = \mu^{(1)} \oplus \mu^{(2)}$ in the case of reflection symmetry and $\tau = 2\mu^{(2)}$ in the case of half-turn symmetry (see also [39]).

Over the complex numbers, the cyclic group $\mathbb{Z}_m = \{0, \dots, m-1\}$ has m 1-dimensional irreducible representations $\mu^{(1)}, \dots, \mu^{(m)}$, where for each $j = 1, \dots, m$ and each $t \in \mathbb{Z}_m$, we have $\mu^{(j)}(t) = \zeta^{t(j-1)}$, with $\zeta = e^{\frac{2\pi i}{m}}$. A straightforward calculation shows that for $m \geqslant 3$, the standard representation τ of $\mathbb{Z}_m$ from Example A.1 decomposes as $\tau = \mu^{(2)} \oplus \mu^{(m)}$ (see e.g. [39, 2]).

The dihedral group $D_4 = \mathbb{Z}_2 \times \mathbb{Z}_2 = \{(0,0), (1,0), (0,1), (1,1)\}$ has four 1-dimensional irreducible representations $\mu^{(00)}, \mu^{(01)}, \mu^{(10)}, \mu^{(11)}$, which are defined by $\mu^{(j_1 j_2)}((t_1, t_2)) = (-1)^{j_1 t_1 + j_2 t_2}$ for $0 \leqslant j_1, j_2 \leqslant 1$ and $(t_1, t_2) \in D_4$. It is again easy to see that the representation τ of D_4 decomposes as $\tau = \mu^{(10)} \oplus \mu^{(01)}$.

Finally, for all $m \geqslant 3$, the representation τ of D_{2m} is an irreducible 2-dimensional representation over the complex numbers [2].

The tensor product of two G-modules (V_0, ρ_0) and (V_1, ρ_1) is the G-module $(V_0 \otimes V_1, \rho_0 \otimes \rho_1)$ with the group action

$$(\rho_0 \otimes \rho_1)(g)(x_0 \otimes x_1) = (\rho_0(g)x_0) \otimes (\rho_1(g)x_1)$$

Example A.3 (Permutation Representation). Suppose S is a finite set and $\alpha : G \times S \to S$ is a permutation action on S. Then α extends to a permutation representation on $k^{|S|}$, the vector space with a basis of formal elements of S. If $S = G$ and α is the group action acting by composition, then α is the regular representation.

With the field k equal to $\mathbb{R}$ or $\mathbb{C}$ and the group G finite, there are only finitely many irreducible representations of G up to isomorphism [29]. We label these irreducible

G-modules as $(k^{n_1}, \mu^{(1)}), \ldots, (k^{n_m}, \mu^{(m)})$ where n_i is the dimension of the i-th irreducible representation and m is the number of conjugacy classes of G. It is customary for the first irreducible $(k^{n_1}, \mu^{(1)})$ to be trivial, meaning $n_1 = 1$ and $\mu^{(1)}(g) = 1$ for every element $g \in G$. Every G-module can be uniquely decomposed as a direct sum of irreducible representations up to isomorphism [29].

Theorem A.4 ([29])**.** *Let $\phi : (V, \rho) \to (W, \eta)$ be a G-homomorphism. The subspaces $\ker \phi \subset V$ and $im\, \phi \subset W$ are G-submodules under the action of ρ and η. Likewise, the cokernel $W/im\, \phi$ is a G-quotient space under η.*

This theorem is utilized in the following fundamental lemma.

Lemma A.5 ((Partial) Schur's Lemma [29])**.** *Suppose (V, ρ) and (W, η) are irreducible G-modules over the field $\mathbb{R}$ or $\mathbb{C}$. If $\phi : (V, \rho) \to (W, \eta)$ is a G-homomorphism then ϕ is an isomorphism or the zero map.*

Following Schur's Lemma every G-module (V, ρ) is equivalent and isomorphic to a unique direct sum of irreducible G-modules. For each irreducible representation $\mu^{(j)}$ of G, let $(V^{(j)}, \rho^{(j)})$ denote the G-submodule of (V, ρ) isomorphic to the direct sum of the integer number $N^{(j)}(\rho)$ of irreducible G-submodules $(k^{n_j}, \mu^{(j)})$ that are factors of (V, ρ). It follows that

$$(V, \rho) \cong (V^{(1)}, \rho^{(1)}) \oplus \cdots \oplus (V^{(m)}, \rho^{(m)}). \tag{42}$$

Suppose $V \cong V_0 \oplus V_1$ and $W \cong W_0 \oplus W_1$ are two G-modules and constituent G-submodules. Further, suppose $\phi_0 : V_0 \to W_0$ and $\phi_1 : V_1 \to W_1$ are two G-homomorphisms. We write $\phi_0 \oplus \phi_1 : V_0 \oplus V_1 \to W_0 \oplus W_1$ for the combined G-homomorphism, represented by a block diagonal matrix

$$\phi_0 \oplus \phi_1 = \begin{bmatrix} \phi_0 & 0 \\ 0 & \phi_1 \end{bmatrix}$$

in some basis $\mathscr{B}_{V_0} \cup \mathscr{B}_{V_1}$ for the domain and a basis $\mathscr{B}_{W_0} \cup \mathscr{B}_{W_1}$ for the codomain.

We say an ordered basis $\mathscr{B} = (b_1, \ldots, b_N)$ for a G-module V is *adapted* if:

- $b_\ell \in \mathscr{B}$ implies that $b_\ell \in V^{(j)}$ for some (j).
- If $b_\ell, b_{\ell'} \in \mathscr{B}$ with $b_\ell \in V^{(j)}$, $b_{\ell'} \in V^{(t)}$ and $j < t$, then $\ell < \ell'$.

Letting $\mathscr{B}^{(j)}$ denote a basis for $V^{(j)}$, it follows that an adapted basis for V is an ordered union of bases $\mathscr{B}^{(1)} \cup \cdots \cup \mathscr{B}^{(m)}$. We say that a vector $x \in V$ is $\mu^{(j)}$-*symmetric* if x is an element of the subspace $V^{(j)}$, or equivalently x is a linear combination of basis vectors in $\mathscr{B}^{(j)}$.

Theorem A.6 ([29])**.** *Suppose G is finite and the field k is $\mathbb{R}$ or $\mathbb{C}$. Every G-homomorphism $\phi : (V, \rho) \to (W, \eta)$ decomposes as a direct sum of G-homomorphisms $\phi^{(1)} \oplus \cdots \oplus \phi^{(m)}$ over irreducibles with*

$$\phi^{(j)} : V^{(j)} \to W^{(j)}.$$

In particular, the matrix $\phi^{(1)} \oplus \cdots \oplus \phi^{(m)}$ is block diagonal with respect to adapted bases of V and W.

Proof. This is a direct consequence of Schur's Lemma A.5. □

Theorem A.7. *Fix a sequence of G-modules*

$$\cdots \to V_3 \xrightarrow{\phi_3} V_2 \xrightarrow{\phi_2} V_1 \xrightarrow{\phi_1} V_0 \xrightarrow{\phi_0} V_{-1} \to \ldots . \tag{43}$$

where maps ϕ_i are G-homomorphisms. For any irreducible representation $\mu^{(j)}$ of G, there is a well-defined sequence of G-submodules

$$\cdots \to V_3^{(j)} \xrightarrow{\phi_3^{(j)}} V_2^{(j)} \xrightarrow{\phi_2^{(j)}} V_1^{(j)} \xrightarrow{\phi_1^{(j)}} V_0^{(j)} \xrightarrow{\phi_0^{(j)}} V_{-1}^{(j)} \to \ldots . \tag{44}$$

where $V_i \cong V_i^{(1)} \oplus \cdots \oplus V_i^{(m)}$ are isomorphic G-modules and ϕ_i is equivalent to the map $\phi_i^{(1)} \oplus \cdots \oplus \phi_i^{(m)}$ in an adapted basis. Moreover, if sequence (43) is exact then sequence (44) is exact for every index (j).

Proof. By Theorem A.6 each map ϕ_i is equivalent to the map $\phi_i^{(1)} \oplus \cdots \oplus \phi_i^{(m)}$ in some adapted basis for V_i. Specifically the image of $\phi_i^{(j)}$ is contained in $V_{i-1}^{(j)}$, meaning the composition $\phi_{i-1}^{(j)} \circ \phi_i^{(j)}$ is well defined.

Suppose that sequence (43) is exact and fix an index i. For $j \neq t$ it must be true that $\ker \phi_i^{(j)} \cap \ker \phi_i^{(t)} = 0$. Thus we have equalities

$$\ker \phi_i^{(1)} \oplus \cdots \oplus \ker \phi_i^{(m)} = \ker \phi_i = \operatorname{im} \phi_{i+1} = \operatorname{im} \phi_{i+1}^{(1)} \oplus \cdots \oplus \operatorname{im} \phi_{i+1}^{(m)}$$

of the G-submodule of V_i. It is also true for $j \neq t$ that $\ker \phi_i^{(j)} \cap \operatorname{im} \phi_i^{(t)} = 0$. Therefore we have an equality of G-submodules $\ker \phi_i^{(j)} = \operatorname{im} \phi_{i+1}^{(j)}$ for each (j) and the sequence (44) is exact. □

We conclude this brief exposition on group representations with a comment on characters. The *character* of a (real or complex) representation ρ is a class function $\chi_\rho : G \to \mathbb{C}$ given by the traces

$$\chi_\rho(g) = \operatorname{trace}(\rho(g)).$$

The *degree* of a character χ_p is the dimension of the representation ρ. Characters are invariants of equivalent representations and hence are basis independent. It is useful to think of the character as a vector $\chi(\rho) \in \mathbb{C}^{|G|}$ where each coordinate is the trace of the matrix $\rho(g)$ (in some basis). Two group elements g_0 and g_1 are *conjugate* if there exists some $h \in G$ such that $g_0 = h^{-1} g_1 h$. The traces of conjugate elements g_0 and g_1 are equal, and hence any *character table* only needs to list a representative from each conjugacy class (noting its multiplicity). An example of a character table is shown in Figure 7.

The following well-known identities then hold for any two representations ρ_1 and ρ_2:

$$\chi(\rho_0 \oplus \rho_1)(g) = \chi(\rho_0)(g) + \chi(\rho_1)(g) \tag{45}$$

$$\chi(\rho_0 \otimes \rho_1)(g) = \chi(\rho_0)(g) \cdot \chi(\rho_1)(g). \tag{46}$$

Moreover, if ρ_0 and ρ_1 are two representations of a finite group G then ρ_0 is equivalent to ρ_1 if and only if $\chi_0 = \chi_1$ [29].

It is well known that the characters of the irreducible representations of a finite group G form a basis for the *dual group* $\hat{G}$ of class functions $G \to \mathbb{C}$ [29]. This allows characters to be decomposed, as shown in Theorem A.9, via the *character inner product*

$$\langle \chi_0, \chi_1 \rangle = \frac{1}{|G|} \sum_{g \in G} \chi_0(g) \cdot \overline{\chi_1(g)} \tag{47}$$

where $\overline{\chi_1(g)}$ is the complex conjugate of $\chi_1(g)$.

Theorem A.8 (Character Orthogonality [29])**.** *Over any finite group G and any two irreducible representations $\mu^{(j)}$ and $\mu^{(t)}$, the following holds:*

$$\langle \chi(\mu^{(j)}), \chi(\mu^{(t)}) \rangle = \begin{cases} 1 & \text{if } j = t \\ 0 & \text{if } j \neq t \end{cases} \tag{48}$$

The characters $\chi(\mu^{(j)})$ from Theorem A.8 are *irreducible characters* and can be looked up in standard references on representation theory [2].

Theorem A.9 (Character Decomposition [29])**.** *Let G be a finite group and χ be the character of a representation ρ of G. Then $\chi(\rho)$ can be uniquely decomposed into a linear combination of irreducible characters*

$$\chi(\rho) = \sum_{(j)} N^{(j)}(\rho) \cdot \chi(\mu^{(j)}) \tag{49}$$

where $N^{(j)}(\rho) = \langle \chi(\rho), \chi(\mu^{(j)}) \rangle$.

These facts make character theory an essential tool for computing and decomposing into G-submodules.

Appendix B. Fully Worked Example

In this section we demonstrate the full process of decomposing chain and homology spaces of a cellular cosheaf into constituent components for each irreducible representation. Due to the considerable complexity, a minimal framework has been selected which has two degrees of self-stress each with a different symmetry type. The framework is pictured in Figure 8 top-left with all cell indices labeled.

The nodes of the "diamond framework" $\mathcal{F}$ in Figure 8 top-left are located at coordinates $(0, \pm 3), (\pm 3, 0)$ and $(\pm 1, 0)$. There are six vertices and eleven edges, so the cosheaf boundary map ∂ of $\mathcal{F}$ (i.e. the equilbrium matrix of $\mathcal{F}$) is a size 12×11 matrix (with cells ordered as in Figure 8, with the x-coordinate of vertex stalks preceding the y-coordinate).

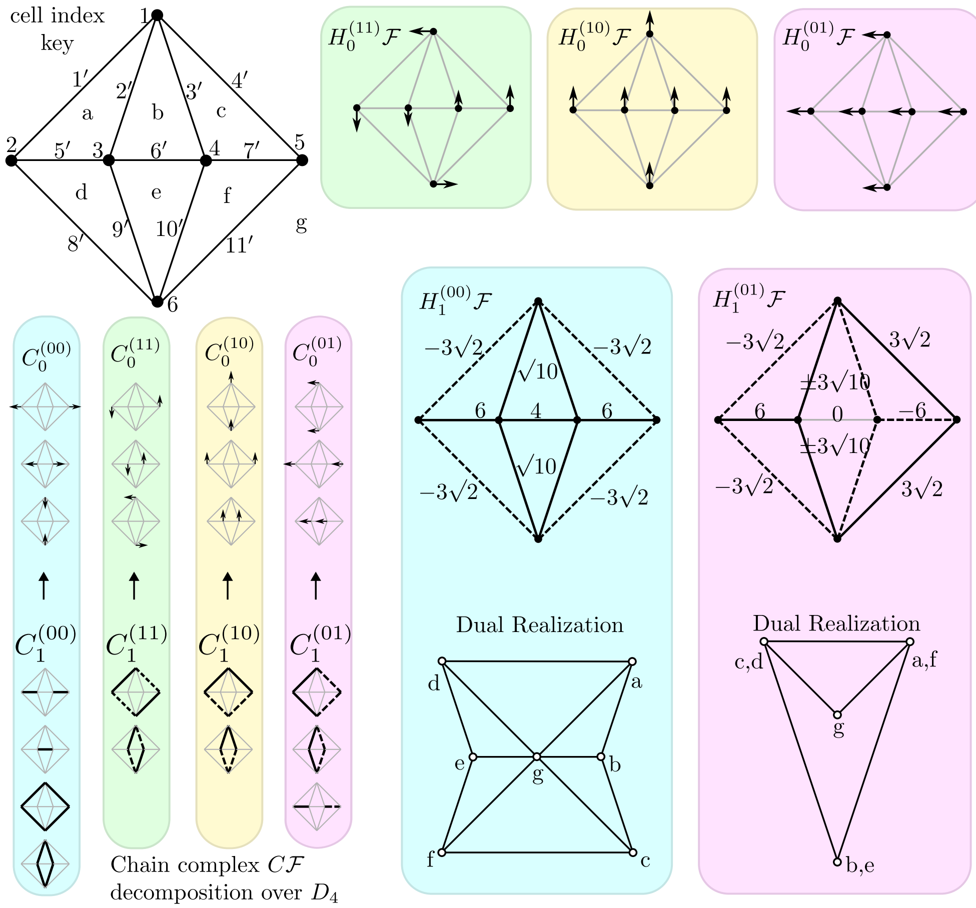

Figure 8: A framework with D_4 symmetry. Cells are labeled (top-left) with numbers i indexing vertices, j' indicating edges and letters indexing faces. The chain complex for the force cosheaf $C\mathcal{F}$ is decomposed by irreducible representations (bottom-left) where the basis vectors of $C_1^{(ij)}$ and $C_0^{(ij)}$ are visually pictured. We see that the matrices $\partial^{(ij)}$ are matrices of size 3×4, 3×2, 3×2 and 3×3. One may then find generators for the homology spaces, pictured (right). Above are the rotational and translational infinitesimal motions of the framework. In the bottom-right are the symmetric self-stresses and their corresponding dual reciprocal frameworks. The values written on the edges are a scalar multiple of each generating self-stress; solid and dashed lines indicate tension/compression. Since point coordinates may overlap in the dual realizations, some nodes and edges might not be visible in the drawing.

$$\partial = \begin{bmatrix} 3 & 1 & -1 & -3 & 0 & 0 & 0 & 0 & 0 & 0 & 0 \\ 3 & 3 & 3 & 3 & 0 & 0 & 0 & 0 & 0 & 0 & 0 \\ -3 & 0 & 0 & 0 & -2 & 0 & 0 & -3 & 0 & 0 & 0 \\ -3 & 0 & 0 & 0 & 0 & 0 & 0 & 3 & 0 & 0 & 0 \\ 0 & -1 & 0 & 0 & 2 & -2 & 0 & 0 & -1 & 0 & 0 \\ 0 & -3 & 0 & 0 & 0 & 0 & 0 & 0 & 3 & 0 & 0 \\ 0 & 0 & 1 & 0 & 0 & 2 & -2 & 0 & 0 & 1 & 0 \\ 0 & 0 & -3 & 0 & 0 & 0 & 0 & 0 & 0 & 3 & 0 \\ 0 & 0 & 0 & 3 & 0 & 0 & 2 & 0 & 0 & 0 & 3 \\ 0 & 0 & 0 & -3 & 0 & 0 & 0 & 0 & 0 & 0 & 3 \\ 0 & 0 & 0 & 0 & 0 & 0 & 0 & 3 & 1 & -1 & -3 \\ 0 & 0 & 0 & 0 & 0 & 0 & 0 & -3 & -3 & -3 & -3 \end{bmatrix} \tag{50}$$

We see the boundary equation of the force cosheaf (4) is reflected in each pair of rows of line (50). Moreover in each column we see that even indexed terms (x-coordinates) and odd indexed terms (y-coordinates) are equal in magnitude but opposite in sign. This reflects that each edge exerts an equal and opposite force on the two vertices it connects.

We now turn to the D_4 group action on the framework, generated by a rotation r and a reflection s in the horizontal axis (so $s \cdot 1 = 6$). Not only are the vertex and edge indices permuted but the stalks themselves are also mixed in the manner indicated in Figure 4 for a square. The combined action on 0-chains is $\rho_0 = \alpha_0 \otimes \tau$ where $\otimes$ is the Kronecker product, α_0 is the permutation representation of the vertex set (recall Example A.3), and τ is the standard representation on $\mathbb{R}^2$ as described in Example A.1:

$$\tau(r) = \begin{bmatrix} -1 & 0 \\ 0 & -1 \end{bmatrix}, \quad \tau(s) = \begin{bmatrix} 1 & 0 \\ 0 & -1 \end{bmatrix}. \tag{51}$$

The representation $\rho_1 = \alpha_1$ over the space $C_1\mathcal{F}$ is simply the permutation representation of the edge set. In the literature, the representations ρ_0 and ρ_1 are also known as the "external" and "internal" representation, respectively (see e.g. [19, 10, 38, 40]).

One can confirm that $\rho_0(g)\partial = \partial\rho_1(g)$ for each group element $g \in D_4$ so that $(\mathcal{F}, \rho)$ satisfies the conditions in Definition 3.2 for a G-cosheaf. By Lemma 3.7 we may decompose the chain complex $C(\mathcal{F}, \rho)$ into a direct sum of chain complexes

$$C(\mathcal{F}, \rho) \cong C^{(00)} \oplus C^{(11)} \oplus C^{(01)} \oplus C^{(10)},$$

each associated with a different irreducible representation of D_4. For computations we find a concrete basis for each space of chains $C_k^{(ij)}$ for dimensions $k = 0, 1$. To this end, we form the maps

$$\gamma_k^{(ij)} := \sum_{g \in G} \chi(\mu^{(ij)})(g) \cdot \rho_k(g) : C_k\mathcal{F} \to C_k\mathcal{F} \tag{52}$$

where the values of $\chi(\mu^{ij})(g) = \mu^{(ij)}(g)$ are described in Example A.2. It is well known from group representation theory that each matrix $\gamma_k^{(ij)} : C_k\mathcal{F} \to C_k\mathcal{F}$ has range equal to the subspace $C_k^{(ij)}$. So we may now form a list of basis vectors $\mathscr{B}_k^{(ij)}$

that span the image of $\gamma_k^{(ij)}$ (i.e. each space $C_k^{(ij)}$). Under these bases the boundary matrix (50) is equivalent to a block diagonal matrix with (not-necessarily square) blocks $\partial^{(ij)}$ along the diagonal.

A sketch of the decomposition of the chain complex $C\mathcal{F}$ along each irreducible representation is pictured in Figure 8 (left) where we can see the dimensions of each block. From each reduced chain complex $C^{(ij)}\mathcal{F}$ we can obtain the self-stresses and infinitesimal motions corresponding to the symmetry type by resolving the homology equations $H_0^{(ij)}\mathcal{F} = C_0^{(ij)}\mathcal{F}/\operatorname{im}\partial^{(ij)}$ and $H_1^{(ij)}\mathcal{F} = \ker\partial^{(ij)}$. These are pictured in Figure 8 (right).

This decomposition procedure, illustrated above for the force cosheaf, applies analogously to the constant cosheaf $\overline{\mathbb{R}^2}$ and the position cosheaf $\mathcal{P}$. In each case, the homology spaces associated with the reduced chain complexes $C^{(ij)}\mathcal{F}$, $C^{(ij)}\overline{\mathbb{R}^2}$ and $C^{(ij)}\mathcal{P}$ capture the structural features of the framework corresponding to a specific symmetry type described by the irreducible representation $\mu^{(ij)}$.

To find the constituent components of maps between homology spaces one simply projects and embeds with respect to the proper bases of each cosheaf. For instance, to find matrix representations for the connecting morphisms $\vartheta^{(ij)} : H_2^{(ij)}\mathcal{P} \to H_1^{(ij)}\mathcal{F}$, one finds a matrix representation of ϑ in the bases $\mathscr{B}^{(ij)}_{H_1\mathcal{F}}$ and $\mathscr{B}^{(ij)}_{H_2\mathcal{P}}$. This amounts to multiplying a matrix representation of ϑ by change-of-basis matrices whose rows and columns consist of the coordinates of the basis vectors in $\mathscr{B}^{(ij)}_{H_1\mathcal{F}}$ and $\mathscr{B}^{(ij)}_{H_2\mathcal{P}}$ respectively. In forming these maps one must take care that the diagram (18) commutes.

Zoe Cooperband zcooperband@gmail.com

Department of Electrical and Systems Engineering (ESE), GRASP Lab, University of Pennsylvania

Miguel Lopez mlopez3@sas.upenn.edu

Department of Applied Mathematics and Computational Science (AMCS), University of Pennsylvania

Bernd Schulze b.schulze@lancaster.ac.uk

School of Mathematical Sciences, Lancaster University